AD-778 351

LIFTING SURFACE THEORY AND HYDRO-ELASTIC INSTABILITY

S. Tsakonas, et al

Stevens Institute of Technology

Prepared for:

Office of Naval Research

September 1973

DISTRIBUTED BY:

NTIS

National Technical Information Service
U. S. DEPARTMENT OF COMMERCE
5285 Port Royal Road, Springfield Va. 22151

Unclassified

SECURITY CLASSIFICATION OF THIS PAGE (When Data Entered)

AD 778 351

REPORT DOCUMENTATION PAGE		READ INSTRUCTIONS BEFORE COMPLETING FORM
1. REPORT NUMBER SIT-DL-73-1653	2. GOVT ACCESSION NO	3. RECIPIENT'S CATALOG NUMBER
4. TITLE (and Subtitle) Lifting Surface Theory and Hydroelastic Instability		5. TYPE OF REPORT & PERIOD COVERED Final 6. PERFORMING ORG. REPORT NUMBER
7. AUTHOR(s) S. Tsakonas, W.R. Jacobs and M.R. Ali		8. CONTRACT OR GRANT NUMBER(s) N00014-67-A-0202-0032
9. PERFORMING ORGANIZATION NAME AND ADDRESS Davidson Laboratory, Stevens Institute of Technology, Hoboken, N.J. 07030		10. PROGRAM ELEMENT, PROJECT, TASK AREA & WORK UNIT NUMBERS
11. CONTROLLING OFFICE NAME AND ADDRESS Naval Ship Research and Development Center Bethesda, Maryland 20034		12. REPORT DATE September 1973 13. NUMBER OF PAGES 80
14. MONITORING AGENCY NAME & ADDRESS(if different from Controlling Office)		15. SECURITY CLASS. (of this report) Unclassified 15a. DECLASSIFICATION/DOWNGRADING SCHEDULE

16. DISTRIBUTION STATEMENT (of this Report)

Approved for public release; distribution unlimited.

17. DISTRIBUTION STATEMENT (of the abstract entered in Block 20, if different from Report)

18. SUPPLEMENTARY NOTES

Reproduced by
NATIONAL TECHNICAL
INFORMATION SERVICE
U S Department of Commerce
Springfield VA 22151

19. KEY WORDS (Continue on reverse side if necessary and identify by block number)

Hydrofoils, unsteady hydrodynamics, flutter

20. ABSTRACT (Continue on reverse side if necessary and identify by block number)

A brief review is presented of the unsteady lifting surface theory and of the "generalized lift operator" technique of inverting the "downwash" integral equation. The integral equation approach is then employed to predict responses of various foils to pitching oscillations and to forward motion in a regular wave train. The agreement between theoretical predictions and experimental results is good for simple configurations

(cont'd)

DD FORM 1 JAN 73 1473 EDITION OF 1 NOV 65 IS OBSOLETE
S/N 0102-014-6601

Unclassified

SECURITY CLASSIFICATION OF THIS PAGE (When Data Entered)

without appendages, but not in the case of the AG(EH) configuration at low frequencies because the presence of the pod is not taken into account in the theoretical calculations. Although the attempt made to remove the spurious leading-edge singularity in the chordwise pressure distribution before inverting the integral equation is questionable, removal of the singularity after the inversion yields responses consistent with other theoretical and experimental trends. An analysis for hydroelastic instability results in the usual non-conservative flutter speed prediction whether using two-dimensional or three-dimensional theoretical lift and moment values with or without the leading edge singularity, except when removal of the leading-edge singularity is introduced before the numerical inversion of the integral equation. The conservative prediction of flutter speed in the latter case raises some plausible speculations as to the proper mode shapes of the hydrodynamic loading distributions on the foil when at the stage of hydroelastic instability. The enforcement of the "Kutta condition" and/or the existence of the physically unrealizable leading-edge singularity may be questionable at that stage. A set of calculations performed with the inclusion of artificial structural damping indicates that the boundary for hydroelastic instability can be brought into coincidence with experimental values by varying the structural damping g from 0.01 to 0.10 through the range of density ratios.

Report SIT-DL-73-1653

September 1973

LIFTING SURFACE THEORY AND HYDROELASTIC INSTABILITY

by

S. Tsakonas

W. R. Jacobs

M. R. Ali

Prepared for
Hydrofoil Program Office
Naval Ship Research and Development Center
under Office of Naval Research
Contract N00014-67-A-0202-0032
(DL Project 3916/134)

Reproduction of this document in whole or in part is permitted for any purpose of the United States Government.

Approved: _____
Daniel Savitsky
Acting Director

ABSTRACT

A brief review is presented of the unsteady lifting surface theory and of the "generalized lift operator" technique of inverting the "downwash" integral equation. The integral equation approach is then employed to predict responses of various foils to pitching oscillations and to forward motion in a regular wave train. The agreement between theoretical predictions and experimental results is good for simple configurations without appendages, but not in the case of the AG(EH) configuration at low frequencies because the presence of the pod is not taken into account in the theoretical calculations. Although the attempt made to remove the spurious leading-edge singularity in the chordwise pressure distribution before inverting the integral equation is questionable, removal of the singularity after the inversion yields responses consistent with other theoretical and experimental trends. An analysis for hydroelastic instability results in the usual non-conservative flutter speed prediction whether using two-dimensional or three-dimensional theoretical lift and moment values with or without the leading edge singularity, except when revmoval of the leading-edge singularity is introduced before the numerical inversion of the integral equation. The conservative prediction of flutter speed in the latter case raises some plausible speculations as to the proper mode shapes of the hydrodynamic loading distributions on the foil when at the stage of hydroelastic instability. The enforcement of the "Kutta condition" and/or the existence of the physically unrealizable leading-edge singularity may be questionable at that stage. A set of calculations performed with the inclusion of artificial structural damping indicates that the boundary for hydroelastic instability can be brought into coincidence with experimental values by varying the structural damping g from 0.01 to 0.10 through the range of density ratios.

TABLE OF CONTENTS

INTRODUCTION

In a series of hydroelastic studies at Davidson Laboratory[1,2,3,4,5], measured response characteristics and flutter speeds of several two-degree-of-freedom hydrofoil models in two- and three-dimensional flow fields were compared with the corresponding values predicted by two- and three-dimensional theories. In all cases, the flutter speed predictions were non-conservative in the low mass-density ratio range which is of practical interest for hydrofoil craft. Various speculations have been made in an attempt to explain the failure of the theoretical analysis to predict flutter speed correctly. These raise questions as to the proper mechanical and dynamical representation of the model and the adequacy of the lifting surface theory in predicting hydrodynamic effects and suggest as causes failure of the imposed Kutta condition, non-linearity of the phehomenon and, finally, the presence of cavitation at the stage of the flutter speed measurements.

Some of the factors supposed to contribute to the failure of the theoretical analysis have been scrutinized and dismissed in Reference 6 where the conclusion has been reached that the flow separation and cavitation, which are inherent characteristics of the selected profiles, are the sole reason for the non-conservative prediction of flutter speed. The most important conclusion, however, concerns the method suggested by References 7, 8, and 9 where corrections for the lift-curve slope and center of pressure location are introduced in the two-dimensional analysis to bring flutter speed predictions closer to the experimental values. It is shown that the modified strip analysis by Yates[7] is invalid when applied to the Grumman model, the flutter speed predictions being more unconservative than were obtained by the usual two-dimensional strip theory or by three-dimensional theory. The favorable comparison shown in Refs. 8 and 9 between experiments and results of the modified strip method is therefore fortuitous, and this method must be considered inappropriate for general application.

Use of the Yates approach in Ref. 10 in the case of a predominantly bending mode of motion also results in non-conservative flutter speed predictions. No general theory has yet been devised which will predict

accurately the hydroelastic boundary of a hydrofoil executing any mode of motion in the low density-ratio range.

Before final judgment is passed on the effectiveness of the lifting-surface theory in predicting the flutter speed for hydroelastic instability, systematic calculations will be performed to evaluate the hydrodynamic characteristics of foil configurations for which experiments are available. The subjects chosen for study are the main foil of the AG(EH) hydrofoil configuration, for which the systematic and detailed experimental work of O'Neill[11] is available, and the simpler rectangular foils tested by Henry[12].

Unfortunately, the experiments of O'Neill were conducted on the AG(EH) main foil composed of a tapered, swept-back wing with a long spheroidal "pod" whose presence cannot be taken into account in the calculations since no theoretical approach is available to deal with the wing-pod interaction. From the solutions of very specific problems and from experimental evidence, it is established[13,14,15] that the interference of two or more lifting surfaces tends to decrease the total lift, the decrement diminishing with increasing reduced frequency.

The credibility of the lifting-surface theory in predicting the hydrodynamic characteristics is established in the present instance by comparison with the results of experiments[12] and other theoretical calculations[16] conducted for configurations without a pod. The agreement between present calculations and experiments for such configurations is very good throughout the range of frequencies.

On the other hand, systematic calculations performed for the AG(EH) main foil in pitching motion and moving in regular head seas show sizable differences from the experimental measurements[11], especially at low frequencies ($k < 0.5$, reduced frequency based on mean geometric chord) where omission of the wing-pod interaction has the most adverse effect. It can be concluded that the discrepancies are realistic and must be attributed to the presence of the pod.

Before using the lift and moment responses calculated by lifting surface theory to predict the flutter speed at the stage of hydroelastic

instability, the influence of the physically unrealizable leading-edge singularity of the chordwise pressure distribution has been investigated. It is known that the linearized lifting surface theory introduces a "square-root" singularity at the leading edge which, though integrable, is nevertheless spurious. This singular behavior is exhibited in the first term ($\cot(\theta/2)$) of the Birnbaum chordwise distribution used in both two- and three-dimensional theory, in steady and unsteady flow fields. The fact that the singular behavior is a localized phenomenon suggested use of the correction factor derived under two-dimensional flow conditions by Van Dyke[17] and Lighthill[18] for removal of the singularity.

Application of this correction factor to the Birnbaum distribution to remove the singular behavior before the inversion of the surface integral equation has yielded results inconsistent with the measurements. This confirms the well-known fact that the linearized theory requires the presence of the leading-edge singularity. On the other hand, removal of the leading-edge singularity after the solution, resulting in loading distributions with finite values at the leading edge, modifies the hydrodynamic forces and moments but only to a small extent.

With hydrodynamic information thus available from the lifting surface theory, either with or without the correction factor for removal of the leading edge singularity, an analysis has been conducted of the hydroelastic instability of two simple hydrofoil configurations with well-defined modes of oscillation for which experimentally determined flutter speeds are available[5].

The predicted flutter speed is non-conservative whether the hydrodynamic information is obtained by two-dimensional or three-dimensional theory uncorrected or corrected by removal of the leading-edge singularity after the inversion of the integral equation. In contrast, when that singularity is removed before the inversion, a conservative flutter speed prediction is achieved. This, of course, raises questions as to the validity of some of the basic assumptions of lifting surface theory at the stage of hydroelastic instability: questions as to the proper mode shapes for the loading distribution at this stage, about the presence of a leading-

edge singularity and/or enforcement of the "Kutta condition". It is to be remembered, however, that inversion of the integral equation with modified chordwise mode shapes yields hydrodynamic forces and moments inconsistent with the trend of experiments and other theoretical calculations.

Inclusion of artificial structural damping brings the over-conservative prediction of the hydroelastic boundary in the latter case into coincidence with that of experiment.

This research was sponsored by the Hydrofoil Program Office of the Naval Ship Research and Development Center under Office of Naval Research Contract N00014-67-A-0202-0032.

WING THEORY

A. The Integral Equation

The surface integral equation relating the lift and incident velocity distributions on a wing of finite aspect ratio immersed in an incompressible ideal fluid is derived by means of the acceleration-potential method with the usual linearizing assumptions (small perturbations, thin surfaces). The equation can be written as

$$W(x,y,z;\omega) = \iint_S \Delta p(\xi,\eta,\zeta;\omega) K(x,y,z;\xi,\eta,\zeta;\omega)\, dS \qquad (1)$$

where

x,y,z / ξ,η,ζ = Cartesian coordinates of control and loading points, respectively

ω = oscillation frequency, rad/sec.

S = wing surface, $ft.^2$

W = incident velocity distribution normal to the wing surface, fps

Δp = unknown pressure on wing, lb/ft^2 (pressure jump across the lifting surface, i.e., $\Delta p = p_+ - p_-$)

K = kernel function representing the velocity induced on the control point (x,y,z) by an oscillatory load of unit amplitude at (ξ,η,ζ) of the wing, ft/lb-sec.

The wing and coordinate systems are shown in the following sketch:

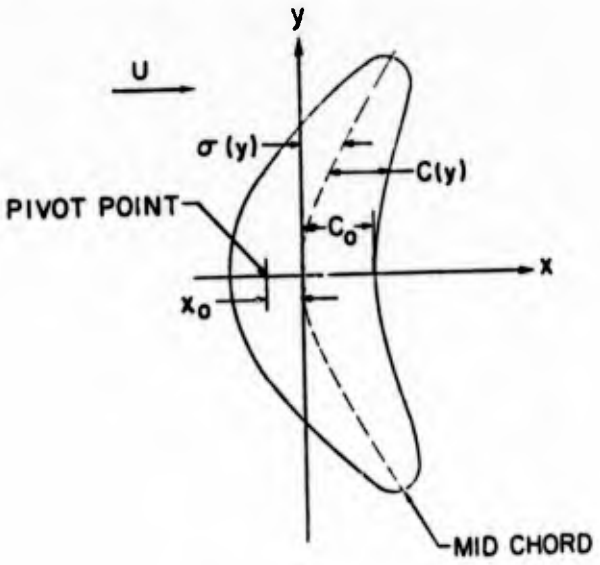

Since the wing is assumed to be thin, z and ζ approach zero. On the surface, shifting the origin to the pivot point,

$$x = \varepsilon(y) - c(y)\cos\phi \quad , \quad \xi = \varepsilon(\eta) - c(\eta)\cos\theta \tag{2}$$

where $\varepsilon = \sigma - x_o$ and $0 \le \phi \le \pi$, $0 \le \theta \le \pi$

$\sigma(y), \sigma(\eta)$ = distance from y-axis to the midchord line at a spanwise location of control or loading point

$c(y), c(\eta)$ = semichord at corresponding locations

ϕ, θ = angular chordwise positions of control and loading points, respectively

x_o = distance of pivot point from midchord at root, positive if in positive x-direction (aft)

The oscillatory velocity distribution normal to the wind may be expressed as

$$W(x,y,0,\omega) = W(x,y,0)e^{i\omega t} \tag{3}$$

where ω is angular frequency and, since the pressure on the wing must pulsate with the same angular frequency, it may be expressed as

$$\Delta p(\xi,\eta,0;\omega) = \Delta p(\xi,\eta,0)e^{i\omega t} \tag{4}$$

With these two substitutions, Eq. (1) becomes

$$W(x,y,0) = \iint_S \Delta p(\xi,\eta,0)K(x,y,0;\xi,\eta,0;\omega)\,dS \tag{1a}$$

The kernel K is derived as

$$K = -\frac{1}{4\pi\rho U c_o^2}\left[\lim_{(z-\zeta)\to 0}\left(-\frac{\partial^2}{\partial z^2}\right)\int_{-\infty}^{x}\frac{e^{ik(\tau'-x)}}{R}d\tau'\right] \tag{5}$$

where $R = [(\tau'-\xi)^2 + r^2]^{1/2}$

$r^2 = (y-\eta)^2 + (z-\zeta)^2$

$k = \omega c_o/U$ reduced frequency

c_o = root semichord, ft.

U = free stream velocity, fps

ρ = fluid density, lb-sec^2/ft^4

and all linear dimensions within the brackets of Eq. (5) are fractions of c_o.

If use is made of the trigonometric transformation (2), the surface integral equation (1a) becomes

$$W(\phi,y,0) = \int_0^{\pi}\int_{\eta} c_o L(\theta,\eta,0)K(\phi,y,0;\theta,\eta,0;\omega)\sin\theta d\theta d\eta \tag{6}$$

with $L(\theta,\eta,0) = c(\eta)\Delta p(\theta,\eta,0)$, the loading in lb/ft, and η is a fraction of c_o.

Finally, since 1/R, the reciprocal of the Descartes distance, can be expressed in the form

$$\frac{1}{R} = \frac{1}{\pi}\int_{-\infty}^{\infty} K_o(|u|r)e^{iu(\tau'-\xi)}du \tag{7}$$

where $K_o(x)$ is the modified Bessel function of order zero, the x or ϕ chordwise dependence of the kernel function and the ξ or θ dependence occur in exponential form as $\exp(\pm if_1\cos\phi)$ and $\exp(\pm if_2\cos\theta)$ and thus are separated from each other. This facilitates the chordwise integration of the loading which is approximated by the Birnbaum modes

$$L(\theta,\eta,0) = \frac{1}{\pi}\left[L^{(1)}(\eta)\ \ \Theta(1) + \sum_{\bar{n}=2}^{\infty} L^{(\bar{n})}(\eta)\ \ \Theta(\bar{n})\right] \tag{8}$$

where $\Theta(1) = \cot\theta/2$

$\Theta(\bar{n}) = \sin(\bar{n}-1)\theta,\ \bar{n} > 1$

and $L^{(\bar{n})}$ are the unknown spanwise components of loading, and permits use of the lift-operator technique.

The exponential, $\exp(\pm if_1\cos\phi)$, can be expanded in terms of the orthogonal and complete set of functions $\phi(\bar{m})$, where for $0 \le \phi \le \pi$

$\Phi(1) = 1 - \cos\phi$

$\phi(2) = 1 + 2\cos\phi$

$\phi(\bar{m}) = \cos(\bar{m}-1)\phi,\ \bar{m} > 2$

in the form

$$e^{\pm if_1\cos\phi} \equiv J_o(f_1) + 2\sum_{\lambda=1}^{\infty}(-1)^{\lambda}J_{2\lambda}(f_1)\cos 2\lambda\phi \mp 2i\sum_{\lambda=1}^{\infty}(-1)^{\lambda}J_{2\lambda-1}(f_1)\cos(2\lambda-1)\phi$$

where $J_n(f_1)$ are Bessel functions of the first kind.

The orthogonality property of $\Phi(\bar{m})$ dictates operation on both sides of integral equation (6) by

$$\frac{1}{\pi}\int_0^{\pi} \Phi(\bar{m})\ \{\ \}d\phi \tag{9}$$

which has been named generalized lift operator. For $\bar{m} = 1$, this is the Glauert lift operator of steady airfoil theory. It is to be noted that the left-hand side of the integral equation can be expressed in a Fourier series expansion with complex coefficients $W(y)$ and angular dependence on ϕ.

Reference 19 has shown that, after evaluation of the kernel (Eq. (5) with substitution of Eq. (7) for 1/R), i.e., after integrating with respect to τ', taking the second derivative with respect to z and the limit as $(z-\zeta) \to 0$, and then performing the chordwise θ and ϕ integrations of the integral equations analytically and the spanwise integrations by the collocation method, the integral equation becomes a set of algebraic equations, with the number $\bar{m}$ of equations equal to the number $\bar{n}$ of unknown chordwise modes. These equations are expressed as

$$\bar{W}^{(\bar{m})}(y_i) = \sum_{n=1}^{\bar{n}\ max} \sum_{j=1}^{J} L^{(\bar{n})}(\eta_j)\bar{k}_{ji}^{(\bar{m},\bar{n})}(y_i,\eta_j) \tag{10}$$

where the superscripts $\bar{m}$ and $\bar{n}$ refer to the order of the lift operator and the chordwise mode, respectively, the subscripts i and j refer to control and loading points, respectively, J is the number of equal spanwise strips of length 2β and

$$\bar{m} = 1,2,\ldots,\bar{n}\ max$$
$$j = 1,2,\ldots,J$$
$$i = 1,2,\ldots,J$$

$$\bar{k}_{ji}^{(\bar{m},\bar{n})}(y_i,\eta_j) = \int_{\eta_j-\beta}^{\eta_j+\beta} \bar{K}^{(\bar{m},\bar{n})}(y_i,\eta)d\eta$$

The modified kernel, i.e., after the θ and ϕ integrations, is (see Ref. 19)

$$\bar{K}^{(\bar{m},\bar{n})} = \frac{1}{\pi^2}\int_0^{\pi}\int_0^{\pi} \Theta(\bar{n})\ \Phi(\bar{m})K(\phi,y,0;\theta,\eta,0;\omega)\sin\theta d\theta d\phi$$

$$= -\frac{1}{4\pi\rho U c_o^2 y_o^2}\left[ky_o\ K_1(ky_o)e^{-ik(\varepsilon_i-\varepsilon_j)} I^{(\bar{m})}(kc_i)\Lambda^{(\bar{n})}(kc_j)\right.$$

$$\left. -\frac{i}{\pi}\int_{-\infty}^{\infty}\frac{|u|y_o K_1(|u|y_o)e^{iu(\varepsilon_i-\varepsilon_j)} I^{(\bar{m})}(-uc_i)\Lambda^{(\bar{n})}(-uc_j)du}{k+u}\right] \qquad (11)$$

where $y_o = y_i - \eta_j$, $K_1(x)$ is the modified Bessel function of order 1 and

$$I^{(\bar{m})}(f_1) = \frac{1}{\pi}\int_0^{\pi}\Phi(\bar{m})e^{if_1\cos\phi}d\phi$$

$$\Lambda^{(\bar{n})}(f_2) = \frac{1}{\pi}\int_0^{\pi}\Theta(\bar{n})e^{-if_2\cos\theta}\sin\theta d\theta \qquad (12)$$

Tables of the latter integrals are given in Appendix A.

For the steady-state condition k = 0, the modified kernel becomes

$$\bar{K}^{(\bar{m},\bar{n})}(k=0) = -\frac{1}{4\pi\rho U c_o^2 y_o^2}\left[I^{(\bar{m})}(0)\ \Lambda^{(\bar{n})}(0) -\right.$$

$$\left.\frac{i}{\pi}\int_{-\infty}^{\infty}\frac{|u|y_o}{u}K_1(|u|y_o)I^{(\bar{m})}(-uc_i)\ \Lambda^{(\bar{n})}(-uc_j)du\right] \qquad (13)$$

The singular u-integral exists in the sense of a Cauchy principal value; therefore, its finite contribution can be easily determined. The integration is performed by Simpson's Method.

The integration of $\bar{K}^{(\bar{m},\bar{n})}$ over all elements of the wing or foil span except that which includes $y = \eta$ is performed by a convenient numerical method. In the region where $y_o = |y-\eta| \to 0$, the η-integral has a high-order singularity. Its finite contribution is obtained by using a polynomial approximation of the modified Bessel function valid in a narrow range about $y_o = 0$ and a three-point Gaussian quadrature for the immediately adjacent ranges.

The treatment of the singular u-integral and η-integral is given in Reference 20.

The spanwise loading components $L^{(\bar{n})}(n_j)$, which by the collocation method are assumed constant over each spanwise strip, are obtained by solution of the $\bar{m}$ simultaneous algebraic equations (10). The spanwise loading distribution L(y) follows from Eq. 8 as

$$L(y) = \int_0^{\pi} L(\theta,y,0)\sin\theta d\theta = \frac{1}{\pi}\int_0^{\pi} L^{(1)}(y)(1+\cos\theta)d\theta +$$

$$\frac{1}{\pi}\sum_{\bar{n}=2}^{\bar{n}\,max}\int_0^{\pi} L^{(\bar{n})}(y)\sin(\bar{n}-1)\theta\sin\theta d\theta = L^{(1)}(y) + \frac{1}{2}L^{(2)}(y) \qquad (14)$$

and the lift force is simply

$$L = c_o\int_y L(y)dy = c_o\int_y [L^{(1)}(y) + \frac{1}{2}L^{(2)}(y)]dy \qquad (15)$$

The pitching moment about the pivot point or axis of rotation is obtained from

$$M_p = \frac{c_o^2}{\pi}\int_y\int_0^{\pi}\{L^{(1)}(y)(1+\cos\theta) + \sum_{\bar{n}=2} L^{(\bar{n})}(y)\sin(\bar{n}-1)\theta\sin\theta\}[\varepsilon(y)-c(y)\cos\theta]\cdot d\theta dy$$

where $[\varepsilon(y) - c(y)\cos\theta]$ is the moment arm. Then

$$M_p = c_o^2\int_y \varepsilon(y)[L^{(1)}(y) + \frac{1}{2}L^{(2)}(y)]dy - c_o^2\int_y c(y)[\frac{1}{2}L^{(1)}(y) + \frac{1}{4}L^{(3)}(y)]dy \qquad (16)$$

(In Eqs. (15) and (16), $\varepsilon(y)$, $c(y)$ and y are fractions of c_o.)

B. Incident Velocity Distributions

The oscillatory velocity distribution, Eq. (3), can be the normal components of any imposed velocity. The theoretical development presented in the preceding section has been applied to several unsteady wing problems.

a. Wing in a sinusoidal gust.

In the case of a horizontal wing or foil advancing at constant speed U in a sinusoidal gust, the incident velocity is given by

$$W(x,y,0)e^{i\omega t} = V_o e^{i\omega\left(t - \frac{x}{U}\right)}$$

so that

$$W(x,y,0) = V_o e^{-i\omega\frac{x}{U}} = V_o e^{-ikx} \tag{17}$$

where $k = \omega c_o/U$, reduced frequency of encounter, and x is nondimensionalized on the basis of c_o the root semichord.

Since

$$x = \sigma(y) - c(y)\cos\phi - x_o = \varepsilon(y) - c(y)\cos\phi$$

Eq. (17) becomes

$$W(\phi,y,0) = V_o e^{-ik\varepsilon(y)} e^{-ik\, c(y)\cos\phi}$$

Application of the generalized lift operator yields

$$\bar{W}^{(\bar{m})}(y_i) = V_o e^{-ik\varepsilon_i}\, I^{(\bar{m})}(kc_i) \tag{18}$$

where $I^{(\bar{m})}(kc_i)$ is as defined in Appendix A.

b. Heaving wing.

For the case of the foil performing heaving oscillations $he^{i\omega t}$, the downwash distribution is given by

$$We^{i\omega t} = i\omega h e^{i\omega t} \tag{19}$$

Then

$$W = ikU\frac{h}{c_o}$$

and, after the lift operator is applied,

$$\bar{W}^{(\bar{m})} = ikU\frac{h}{c_o} I^{(\bar{m})}(0) \tag{20}$$

c. Pitching wing

A foil performs oscillations of small amplitude $\alpha_o x\, e^{i\omega t}$ about a pivot point, or axis of rotation. The corresponding downwash distribution is

$$We^{i\omega t} = \alpha_o(U+i\omega x)e^{i\omega t} \tag{21}$$

Then

$$W = \alpha_o U(1+ikx)$$

where now x is a fraction of c_o, or

$$W = \alpha_o U[1+ik\varepsilon(y)-ik\, c(y)\cos\phi]$$

After application of the lift operator, this equation becomes

$$\bar{W}^{(\bar{m})} = \alpha_o U[(1+ik\varepsilon_i)I^{(\bar{m})}(0) - ik\, c_i I_1^{(\bar{m})}(0)] \qquad (22)$$

$I_1^{(\bar{m})}(0)$ is also defined in Appendix A.

d. Submerged wing moving in regular waves

The forces snd moments acting on a wing (foil) which moves in a regular wave system of small amplitude can be studied by means of the present analysis by assuming the incident velocity at the foil is that resulting from the wave train, without distortion due to the presence of the foil.

The velocity potential of the wave is then

$$\Phi_W = -iac_w \exp\frac{2\pi}{\lambda}\{z-h-i[x\cos\gamma-y\sin\gamma-(c_w+U\cos\gamma)t]\} = \phi_{w_o} e^{i\omega_e t} \qquad (23)$$

where $\omega_e = (2\pi/\lambda)(c_w+U\cos\gamma)$ = frequency of encounter

a = wave amplitude

λ = wave length

$c_w = \sqrt{g\lambda/2\pi}$ = wave celerity

U = forward velocity of foil

h = depth of foil below free surface (z=0 at the foil)

γ = angle of wave heading with positive x-axis (γ = 0 for head seas)

The normal velocity W at the foil due to the wave is

$$W = \left.\frac{\partial\Phi_{w_o}}{\partial z}\right|_{z=o} = -ia\,\frac{2\pi c_w}{\lambda} e^{\frac{-2\pi h}{\lambda}} e^{\frac{-i2\pi}{\lambda}(x\cos\gamma-y\sin\gamma)}$$

$$= -ia(\omega_e - \frac{2\pi U}{\lambda}\cos\gamma) e^{\frac{-2\pi h}{\lambda}} e^{\frac{-i2\pi}{\lambda}(x\cos\gamma-y\sin\gamma)} \qquad (24)$$

On setting $k_e = \omega_e c_o/U$ and non-dimensionalizing a, λ, h, x and y by c_o, Eq. (24) is transformed into

$$W = -iaU(k_e - \frac{2\pi\cos\gamma}{\lambda}) e^{\frac{-2\pi h}{\lambda}} e^{\frac{-i2\pi}{\lambda}(x\cos\gamma - y\sin\gamma)} \tag{25}$$

After substituting $x = \sigma(\gamma) - c(y)\cos\phi - x_o = \varepsilon(y) - c(y)\cos\phi$ and applying the generalized lift operator, the normal velocity per nondimensional wave amplitude will be

$$\frac{\bar{w}^{(\bar{m})}}{a} = -iU(k_e - \frac{2\pi\cos\gamma}{\lambda}) e^{\frac{-2\pi h}{\lambda}} e^{\frac{-i2\pi}{\lambda}(-y_i\sin\gamma + \varepsilon_i\cos\gamma)} {}_1(\bar{m})(\frac{2\pi}{\lambda} c_i \cos\gamma) \tag{26}$$

The solution of the integral equation will yield values of lift and moment per nondimensional wave amplitude in this case.

Since k_e and λ are interdependent and k_e alone is required for the right-hand side of the integral equation, the wave length λ is computed from the relation

$$k_e = k_w(k_w F^2 + 1)$$

where k_w = reduced frequency of the wave and F = Froude number based on c_o.

It can be easily shown that the nondimensional wave length is

$$\lambda = \frac{\pi g c_o}{2U^2 k_e^2}\left(1 + \sqrt{1 + \frac{4k_e U^2\cos\gamma}{g c_o}}\right)^2 \tag{27}$$

e. Surface-piercing vertical strut

The present analysis can accommodate a study of a surface-piercing strut moving at high speed in a regular wave train (or executing any mode of motion). It is shown in Appendix B that, at high Froude number, a foil with effective span equal to twice the submerged portion of the strut is hydrodynamically equivalent to the surface-piercing strut, provided that the incident velocity distribution (downwash) is extended asymmetrically with respect to the free surface where the incident velocity is zero. This equivalence is valid in both steady and unsteady flows.

For a vertical strut, the normal velocity W in the positive y-direction due to regular waves is given by (cf Eq. (23))

$$W = \frac{\partial \Phi_w}{\partial y}\Big|_{y=o} = \frac{a2\pi}{\lambda} c_w \sin\gamma \, e^{\frac{2\pi}{\lambda}z'} e^{\frac{-i2\pi}{\lambda} x \cos\gamma} \tag{28}$$

where $z' = 0$ at the free surface and $z' = -h$ at the submerged bottom of the vertical strut. Then, nondimensionalizing on the basis of semichord c_o at the free surface and noting that in this case

$$x = \sigma(z') - c(z')\cos\phi$$

the normal velocity per nondimensional wave amplitude becomes

$$\frac{W}{a} = U\sin\gamma\left(k_e - \frac{2\pi}{\lambda}\cos\gamma\right)\exp\left\{\frac{2\pi}{\lambda}z' - \frac{i2\pi}{\lambda}\cos\gamma[\sigma(z') - c(z')\cos\phi]\right\} \tag{29}$$

On the submerged part of the strut $z' \leq 0$ so that $z' = -|z'|$. With this substitution and, after application of the lift operator, the normal velocity to the strut becomes for each $\bar{m}$

$$\frac{\bar{W}^{(\bar{m})}}{a} = U\sin\gamma\left(k_e - \frac{2\pi}{\lambda}\cos\gamma\right)\exp\left\{-\frac{2\pi}{\lambda}|z'| - i\frac{2\pi}{\lambda}\cos\gamma\sigma(|z'|)\right\} \cdot I^{(\bar{m})}\left(\frac{2\pi}{\lambda}c(|z'|)\cos\gamma\right) \tag{30}$$

with the nondimensional wave length λ given by (27).

The velocity distribution on the *effective* strut will then be given by

$$\frac{\bar{W}^{(\bar{m})}}{a} = \text{[Eq. (30)] for } z' < 0 \text{ (the submerged part of the strut)}$$
$$= 0 \text{ for } z' = 0 \text{ (at the free surface)}$$
$$= -\text{[Eq. (30)] for } z' > 0 \text{ (the upper part of the effective strut)}$$

so that the imposed asymmetry of the velocity distribution is fulfilled.

The spanwise loading components are computed for the assumed double strut which is divided into an odd number of vertical spanwise strips of equal length, the center of the middle one being at the free surface. These loading components are integrated over the submerged part only, to obtain the side force. The rolling moment about the bottom of the strut is the integral of the products of the submerged strip side forces by their moment arms.

In Reference 19, the solution of the surface integral equation presented here, which used the generalized lift operator technique in conjunction with the Birnbaum chordwise modes, was applied to three two-dimensional nonstationary airfoil problems for incompressible flow: 1) a foil advancing at constant speed in a sinusoidal gust, 2) a foil performing heaving oscillation and 3) a foil performing rotational oscillation about the midchord point. It was demonstrated in that reference that the present procedure recaptures the known analytical solutions of those problems.

APPLICATION OF THE COMPUTER PROGRAM

A computer program adaptable to the CDC 6600 high-speed digital computer has been devised for the numerical solution of the surface integral equations of the unsteady, three-dimensional foil problems described earlier. The program follows the development of the preceding sections and parallels the procedure used in the case of a rudder (totally submerged vertical foil) treating the singularities in the same way[20].

A. Rectangular Foils and Surface-Piercing Struts

The numerical procedure and corresponding program have been utilized first to obtain the lift responses of a set of rectangular foils of aspect ratio 1 and 2 moving in a sinusoidal gust, for which cases experimental results are available[21]. Figure 1 compares the values of lift curve slope calculated by the present method with the experimental data and with the results of other theoretical methods. In addition to the theoretical values of low-aspect ratio theory[21] and of Falkner's vortex lattice method[22] which were included in Reference 19, the estimates by Engineering Sciences Data (ESD)[16] are also shown. The results of the present lifting-surface approach are seen to follow the upper limits of the xperimental data whereas the results of Falkner and ESD follow the lower limits.

Figure 2 shows locations of centers of pressure aft of the leading edge versus spanwise position for the same two foils at various reduced frequences k. The center of pressure is given as $\bar{x}/2c_o$ where $2c_o$ is the root chord (constant over the span in the case of rectangular foils) and $\bar{x}$ is computed as the quotient of pitching moment about the midchord by the lift. As is seen, the higher the aspect ratio, the closer the value of $\bar{x}/2c_o$ to the quarterchord line which is the center of pressure of the two-dimensional foil.

The present theoretical approach was also applied to the case of submerged rectangular foils of NACA 64-012 section and different aspect ratios moving at constant speed in regular seas. Figure 3 exhibits the lift response coefficients C_L to unit dimensionless wave amplitude a/c_o versus k_e for such foils of aspect ratio 2 and 4 in regular head seas.

Here $C_L = \frac{L}{2\rho U^2 c_o s_o}$

ρ = density of water

c_o = semichord length

s_o = semispan length

U = foil speed

The calculations are compared with experimental measurements at Davidson Laboratory[12] and with the results of other theoretical methods, two-dimensional theory[23] and a modification given by Reissner and Stevens[24] for high aspect ratio oscillating wings in uniform flow. Figure 4 compares the present theoretical calculations of lift response coefficients for foils of aspect ratio 4 and 6 at two submergences in regular oblique seas with experimental values[12]. These figures show good agreement on the whole between the predictions by the present three-dimensional unsteady lifting-surface theory and the experimental data.

Figure 5 shows the side force response coefficients versus k_e in the case of 2 vertical surface-piercing struts of effective aspect ratios 2 and 4 moving at constant speed in regular oblique waves. The results of the present theory are in fair agreement with the experiments[12].

The agreement between present theoretical results and experimental data is seen to range from very good to satisfactory, the latter classification occurring when the foil is submerged to a depth of only one chord. Since the theory does not take into account free-surface effects, the poorer agreement at the lesser depth must be attributed to this omission.

The generally good correlation between theory and experiment in the case of these foils without appendages serves to establish the credibility of this wing theory and computer program. This needs to be said since in the case of the AG(EH) main foil, which will be considered presently, the experimental results are from tests of the foil attached to a long pod, whereas in the calculations the presence of the pod is completely ignored and hence no hydrodynamic interaction of the foil-pod-strut assembly is considered.

B. AG(EH) Main Foil

Systematic calculations have been performed for the main foil of the AG(EH) hydrofoil which is the subject of a detailed experimental study by O'Neill[11]. The geometry of the foil is exhibited in Figure 6 and the principal characteristics of the main foil and its pod are given in the following table.

Characteristics of Main Foil and Pod

Foil area	*225.0 ft²*
Aspect ratio	*3.0*
Taper ratio	*0.30*
Foil section	*NACA-16 (Mod)*
Maximum thickness ratio t/c	*0.08*
Mean geometric chord, c	*8.65 ft.*
Root chord, $2c_o$	*13.314 ft.*
Maximum diameter of pod	*3.333 ft.*
Length of pod	*26.812 ft.*
Distance of l.e. of pod fwd. of pivot 1	*12.281 ft.*

The calculations were performed for the foil executing pitching motion about a pivot point 0.062c aft of the leading edge of the geometric mean chord and about one 0.32c aft of that leading edge, and for the foil advancing in regular head seas at 14.2 knots and at 20.5 knots.

The results of the pitching motion calculations are exhibited in Figures 7 to 10 in the form of unsteady lift and moment curve slopes versus dimensionless pitching frequency, i.e., reduced frequency k. Figures 7 and 8 present the lift and moment curve slopes respectively when the foil is pitching about the pivot point at 0.062c and Figures 9 and 10 the corresponding results when the foil is pitching about the pivot point at 0.32c. (The results of these calculations are also summarized in Tables Ia and Ib in the columns headed "Without Correction".)

Figure 11 presents the variation with frequency k of the center of pressure location aft of the leading edge of the mean geometric chord, derived from the calculations for the AG(EH) main foil in pitching motion about the different pivot points. It is seen that with increasing fre-

quency, especially when k > 0.2, the center of pressure location for this sweptback and tapered foil moves further away from the leading edge. It is further interesting to note that the calculations exhibit the well-known fact that the center of effort (or pressure) is independent of the pivot point location, thus demonstrating the consistency of the numerical work.

Figure 12 is a comparison of the experimentally and theoretically determined phases by which the lift and pitching moment lead the foil position in pitching motion. In spite of the existing discrepancies between the experimental and theoretical magnitudes seen in Figures 7-10, the phase agreement is excellent.

Calculations have also been done for the main foil of the AG(EH) hydrofoil moving in regular head seas with speeds of 14.2 and 20.5 knots. Results of these computations are presented graphically in Figures 13-16 and tabulated in Table IIa. In Figures 13 and 14, the unsteady lift and hinge moment responses at 14.2 knots are compared with the corresponding experimental results for varying values of dimensionless wave length. Figures 15 and 16 present the results at 20.5 knots.

In Figures 13 and 15, the lift responses are also compared with the results of the two-dimensional theory developed in Appendix C by means of the "Generalized Lift-Operator" technique. The developed expression for lift is identical with those given by Kemp[23] and Leehey[25]. It is seen here that the two-dimensional approach overestimates the lift considerably, as it should, in contrast to what is shown in Reference 11 after a modification for the effect of the horizontal component of wave orbital velocity.

It is apparent from this set of calculations for the AG(EH) mainfoil that there are considerable discrepancies between experimental results and the results of the present three-dimensional theory especially in the lower frequency range. As the frequency increases, the agreement between theory and experiment improves.

When examining Figures 7-16, it should be kept in mind that the experiments were run on an AG(EH) mainfoil composed of a tapered, sweptback wing and a spheroidal "pod" of 3.33 ft. diameter and 26.812 ft. length, whereas the theoretical calculations, using the "lifting surface" approach,

take the entire planform as wing. The pod is thus replaced by a more effective lifting surface (i.e. wing) and this results in larger values of lift than are measured.

Unfortunately, no theoretical approach is available for dealing with the wing-fuselage interaction problem. From the solution of a specific problem, that of delta wing with slender fuselage, and from experimental evidence, it has been established[13,14,15] that the effect of interference of two or more lifting surfaces is to decrease the total lift and that this tendency is diminished with increasing reduced frequency.

For a range of frequency $k \geq 0.5$, there is satisfactory agreement between the results of theory and experiment. Furthermore, at high frequencies the theoretical results increase as k^2, a known trend also exhibited by the experimental results.

It is also to be noted that at $k = 0$ (steady-state) the theoretical results for the main foil without pod are close to values reported by ESD[16] for the tapered, sweptback wing itself.

Attempts have been made to achieve better correlation between theory and experiment by correcting the theoretical results in head seas for the contribution arising from the horizontal component of the wave orbital velocity and by treating the pod as a separate body. Neither correction has substantially diminished the discrepancy.

In the linear theory, the horizontal component of the wave orbital velocity is neglected as small and the main contribution to the lift is considered as coming from the vertical component. When the foil is at zero angle with respect to the forward speed, the contribution of the horizontal component is identically zero. When, however, the foil is placed at an angle α and hence operates with non-zero mean lift, the horizontal component contributes to the loading and thus to the lift and hinge moment. The downwash velocity W imposed on the foil due to a regular wave train, given in Eq. (25), will be modified to include the effect of the horizontal component U_w of the orbital velocity so that the resultant downwash will be given by

$$W - U_w \alpha$$

where in head seas ($\gamma = 0$)

$$U_w = \left.\frac{\partial \Phi w_o}{\partial x}\right|_{z=o} = -a \frac{2\pi}{\lambda} c_w \exp \frac{2\pi}{\lambda} \{-h - ix\}$$

(see Eq. 23). It is apparent that $U_w \alpha << W$ and hence its effect must be small. Calculations have shown the effect of the horizontal component to be within 3-10% of the main contributor. Reference 26 cites the same qualitative results on the basis of both theory and experiments.

In the attempt to determine the lift force exerted by the pod alone moving in regular head seas, the method of Havelock[27] was used. Calculations for a series of wave lengths have shown that the lifting force is small compared to that of the wing alone and could not account for the existing discrepancy between theory and experiments. It is the interference between the pod and the wing that considerably affects its loading distribution and hence its forces and moments.

These systematic calculations performed for various modes of motion show sizable discrepancies from experimental measurements at low frequencies, when theory neglects the pod. In contrast, experiments conducted without the pod are in good agreement with the theoretical results. It could be concluded, therefore, that the discrepancies are realistic and must be attributed to the presence of the pod. Since the pod is an integrated part of any hydrofoil configuration, its presence cannot be ignored in the theoretical development if accurate loading distributions and forces and moments are desired.

REMOVAL OF THE SINGULAR BEHAVIOR OF THE CHORDWISE PRESSURE DISTRIBUTION

The linearized wing theory considers an arbitrary wing cross-section as composed of a symmetrical part corresponding to the thickness distribution and an asymmetrical part associated with a wing of zero thickness. The asymmetrical part contributes to the lift, whereas the symmetrical part contributes nothing to the lifting properties of a wing unless it is nonplanar. Since present interest lies in determining the forces and moments due to the lifting properties of a planar wing or foil and in the question of the "effectiveness" of lifting surface theory in predicting the flutter speed in the study of hydroelastic instability, only the pressure distributions associated with loading will be considered. The loading may be due to the effects of camber, angle of attack, or any other imposed incident velocity.

The linearized thin-wing theory furnishes useful information about the pressure or loading distribution over the foil area; however, it is known to fail near the leading and trailing edges where the basic assumption of small disturbances is violated if there is a stagnation point. At such a point, the pressure distribution exhibits singular behavior which, although integrable, is physically unrealizable. Investigations have been undertaken in the attempt to remove the singular behavior by introducing a proper correction factor depending on the edge geometry.

The singular behavior of the loading distribution is exhibited in the first term, $\cot\theta/2$, of the Birnbaum chordwise distribution which is assumed in both two and three-dimensional theory, in steady and unsteady flow fields. Since the singular behavior is a localized phenomenon, it is conceivable that the method of VanDyke[17] and Lighthill[18] for removing the singularity at a parabolic leading edge in the two-dimensional, steady-state case can be applied in the three-dimensional, steady and unsteady flow cases. Their correction factor will therefore be used to modify the first term of the Birnbaum distribution.

The loading distribution of a foil or wing operating under known steady or unsteady flow conditions is determined through solution of a singular integral equation, the "downwash" integral equation relating the

unknown loading with the known imposed velocity. Although it is known that the solution requires a square-root singular behavior at the leading edge of the foil[28], an attempt has also been made to remove the leading-edge singularity before the inversion of the integral equation. It was thought that, since the modification of the singularity is localized, it would have minimal effect on the solution of the equation and that this approach might lead to faster convergence of the chordwise modes and to a smoother pressure distribution. However, this approach leads to results inconsistent with the trend of experiments and other theoretical calculations. It is therefore concluded that the approach of removing the leading-edge singularity before the inversion of the integral equation should be used with caution.

On the other hand, removal of the leading-edge singularity after the solution of the integral equation yields results which show the same overall picture as those with no correction, but secure a finite pressure at the leading edge.

The simplest edge correction to be applied to the linearized solution for incompressible flow is that given by VanDyke and Lighthill. Their simple rule for obtaining a solution uniformly valid near the edge is

$$\bar{C}_p = \frac{s}{s + \rho_o/2} C_{p_1} \tag{31}$$

where C_{p_1} = pressure coefficient according to the first-order thin airfoil theory

s = $(1-\cos\theta)/2$ = chordwise location from the leading edge, in terms of chord length

ρ_o = leading-edge radius of the section in terms of chord length

This correction falsely implies that the nose exerts an influence at remote points and to this extent it fails to give a "uniformly valid" solution. However, the influence is small and the correction procedure is so simple as to be exceedingly appealing for use in modifying results of linearized lifting surface theory.

If the correction factor is applied to all chordwise modes of Eq. (8), then the loading function can be written as

$$L(\theta,\eta,0) = \left[\frac{1-\cos\theta}{1+\rho_o-\cos\theta}\right]\frac{1}{\pi}\left\{L^{(1)}(\eta)\cot\frac{\theta}{2} + \sum_{\bar{n}+2}^{\infty} L^{(\bar{n})}(\eta)\sin(\bar{n}-1)\theta\right\} \qquad (32)$$

where $L^{(\bar{n})}(\eta)$ are the spanwise loading components to be determined by the solution of the integral equation. If the leading-edge singularity is removed before the solution, the $\Lambda^{(\bar{n})}$ functions become, instead of those given in Eq. (12),

$$\Lambda^{(1)}(f_2) = \frac{1}{\pi}\int_o \frac{\sin^2\theta}{1+\rho_o-\cos} e^{-if_2\cos\theta} d\theta$$

$$\Lambda^{(\bar{n})}(f_2) = \frac{1}{\pi}\int^{\pi} \frac{1-\cos\theta}{1+\rho_o-\cos\theta} e^{-if_2\cos\theta} \sin(\bar{n}-1)\theta\sin\theta d\theta \quad \bar{n} > 1 \qquad (33)$$

These expressions are evaluated in Appendix D.

Once the spanwise loading coefficients $L^{(\bar{n})}(\eta)$ are determined, either by using Eq. (8) for the uncorrected Birnbaum modes if the singularity is to be removed after the solution, or Eq. (33) for the modified modes if the singularity is to be removed before the solution, the spanwise loading distribution with edge correction is obtained, using Eq. (32), from

$$L(\eta) = \int_o^{\pi} L(\theta,\eta,0)\sin\theta d\theta = L^{(1)}(\eta)\,\Lambda^{(1)}(0) + \sum_{\bar{n}=2}^{\infty} L^{(\bar{n})}(\eta)\,\Lambda^{(\bar{n})}(0) \qquad (34)$$

where $\Lambda^{(\bar{n})}(0)$ is obtained from Eq. (33) with $f_2 = 0$ (see Appendix D). The values for the first four $\bar{n}$ modes are:

$$\Lambda^{(1)}(0) = 1 + \rho_o - \sqrt{2\rho_o+\rho_o^2}$$

$$\Lambda^{(2)}(0) = \frac{1}{2} - \rho_o - \rho_o^2 + \rho_o\sqrt{2\rho_o+\rho_o^2}$$

$$\Lambda^{(3)}(0) = -\rho_o - 4\rho_o^2 - 2\rho_o^3 + 2(\rho_o+\rho_o^2)\sqrt{2\rho_o+\rho_o^2} \qquad (35)$$

$$\simeq -\rho_o - 4\rho_o^2 + 2\rho_o\sqrt{2\rho_o+\rho_o^2}$$

$$\Lambda^{(4)}(0) = -\rho_o - 9\rho_o^2 - 12\rho_o^3 - 4\rho_o^4 + (3\rho_o + 8\rho_o^2 + 4\rho_o^3)\sqrt{2\rho_o+\rho_o^2}$$

$$\simeq -\rho_o - 9\rho_o^2 + 3\rho_o\sqrt{2\rho_o+\rho_o^2}$$

In the limiting case as $\rho_o \to 0$

$$\Lambda^{(1)}(f_2) \to J_o(f_2) - iJ_1(f_2) + O(\rho_o^{1/2}) \to J_o(f_2) + iJ_1(f_2)$$

$$\Lambda^{(\bar{n})}(f_2) \to \frac{(-1)^{(\bar{n}-2)}}{2}\left[J_{\bar{n}-2}(f_2) + J_{\bar{n}}(f_2)\right]$$

and $\Lambda^{(1)}(0) \to 1$

$$\Lambda^{(2)}(0) \to \frac{1}{2}$$

$$\Lambda^{(\bar{n})}(0) \to 0 \quad , \quad \bar{n} > 2$$

thus recapturing the values obtained without correction of the Birnbaum chordwise modes.

In summary, Eqs. 8, 12 and 14 are used for a solution of the integral equation without correction, Eqs. 32, 33 and 34 are used when the correction for leading edge singularity is made before the solution, and Eqs. 32, 12 and 34 are used when the correction is made after the solution.

The various solutions of the integral equation, "without correction", "with correction for l.e. singularity before solution," and "with correction for l.e. singularity after solution", are presented in Tables Ia and Ib for the lift and moment curve slopes of the AG(EH) main foil in pitching motion and in Tables IIa, IIb and IIc for the lift and hinge moment coefficients per unit dimensionless wave amplitude in head seas. It is seen that the results of calculations with correction before solution are for the most part quite large compared with those without correction at low reduced frequencies, where the latter are themselves high compared with experimental measurements. The results of the calculations with correction for the leading edge singularity after the inversion of the integral equation are close to those without any correction.

In fact, the closeness of the calculations with correction after solution to the uncorrected results depends on the leading-edge radius ρ_o. If the section is quite thick, the formula (31) for the linearized correction for the leading-edge singularity is valid only very close to the leading edge and should not be used for evaluating the lifting properties of

the section but only for evaluating the maximum finite value of the loading at the leading edge.

In the case of nonplanar lifting surfaces such as propeller blades, the correction before the solution leads to results even more inconsistent with known trends, further evidence of the need for the presence of the leading-edge singularity in the solution. It is therefore concluded that the approach of removing the l.e. singularity before the inversion of the integral equation should be used cautiously.

The scheme of removing the singularity after the solution yields a pressure distribution due to loading with finite value at the leading edge which is useful information for cavitation studies.

Figure 17 is a sample of chordwise pressure distributions due to loading for the AG(EH) main foil with NACA-16(MOD) cross-section, when executing pitching motion of *unit amplitude*. The calculations of $C_p = P/\frac{1}{2}\rho U^2$ per radian were performed using all three schemes. Figure 17 is for a reduced frequency $k = \omega b/U = 0.065$ at the spanwise location $y = .125$ of the semi-span from the root chord but is typical of the results for any frequency and spanwise location. It is seen that the pressure distributions per radian of pitch without correction and with correction for l.e. singularity applied after the solution are very close except within 2.5% of the chord from the leading edge. In contrast, when the l.e. singularity is removed before the inversion of the integral equation, the pressure distribution is similar in trend but quite different in magnitude.

ANALYSIS OF HYDROELASTIC INSTABILITY

In all hydroelastic studies, the flutter speed predictions, whether by three or two-dimensional theory, have been non-conservative in the low mass-density-ratio range which is of practical interest for hydrofoil craft. Various speculations have been made in an attempt to explain the failure of the theoretical analysis and to suggest corrections but none has been of general nature or wide applicability.

A new attempt will be made here to predict the instability boundary and flutter speed by using the results of the lifting surface theory obtained through the inversion of the singular integral equation by means of the "generalized lift operator" technique. Before final judgment is passed on the effectiveness of lifting surface theory in predicting the flutter speed, calculations will also be made using the two sets of hydrodynamic forces and moments obtained when the leading edge singularity is removed before the inversion of the surface-integral equation and after the inversion.

The subjects of the hydroelastic study are two rectangular foils of aspect ratio 2 and 4 and with NACA-0012 cross-section, having two degrees of freedom (in pitching and heaving). The results of flutter experiments on these foils are presented in Reference 5.

The equations of motion for foils with the two degrees of freedom, heaving and pitching, are given in Reference 1 as

$$\mu\left[1 - \left(\frac{\omega_h}{\omega_\alpha}\right)^2 \left(\frac{\omega_\alpha}{\omega}\right)^2\right] h_o e^{i\omega t} + \mu\beta x_\alpha \alpha_o e^{i\omega t} = L/\pi\rho b^3\omega^2$$

$$\mu\beta x_\alpha h_o e^{i\omega t} + \mu r_\alpha^2\left[1 - \left(\frac{\omega_\alpha}{\omega}\right)^2\right]\alpha_o e^{i\omega t} = M/\pi\rho b^4\omega^2 \qquad (36)$$

where b = semichord

$\mu = m/\pi\rho b^2$ = density ratio

$\beta = m_\alpha/m$ = coupling mass ratio

m = total oscillating mass per unit span $(=m_\alpha + m_h)$

m_α = mass of rotating parts per unit span

m_h = mass of translating parts per unit span

x_α = dimensionless distance in semichords from the rotational axis to the c.g. of m_α, positive if the c.g. is aft

r_α = dimensionless radius of gyration about rotational axis ($r_\alpha^2 = I_\alpha/mb^2$)

I_α = mass polar moment of inertia of rotating parts about the rotational axis, per unit span

h_o = amplitude of simple harmonic translatory motion

α_o = amplitude of simple harmonic rotary motion

ω_h = uncoupled natural frequency in translation

ω_α = uncoupled natural frequency in rotation

ω = circular frequency of oscillatory motion

L,M = unsteady hydrodynamic lift and moment, per unit span

When the rotational axis is at the quarterchord, as it was in the experiments, the lift and moment per unit span are

$$L = \rho\pi b^3\omega^2 \{L_h h_o + L_\alpha \alpha_o\} e^{i\omega t}$$
$$M = \rho\pi b^4\omega^2 \{M_h h_o + M_\alpha \alpha_o\} e^{i\omega t} \qquad (37)$$

where the subscripts h and α refer to the translatory and rotary motions, respectively, and L_h, L_α, M_h, M_α are dimensionless unsteady hydrodynamic coefficients and complex functions of reduced frequency $k = \omega b/U$. After substituting Eqs. (37) for L and M in Eqs. (36), the latter are seen to be homogeneous, complex, simultaneous linear algebraic equations in the unknown amplitudes h_o and α_o:

$$\{\mu[1 - (\frac{\omega_h}{\omega_\alpha})^2 (\frac{\omega_\alpha}{\omega})^2] + L_{hr} + iL_{hi}\}h_o + \{\mu\beta x_\alpha + L_{\alpha r} + iL_{\alpha i}\}\alpha_o = 0$$
$$\{\mu\beta x_\alpha + M_{hr} + iM_{hi}\}h_o + \{\mu r_\alpha^2[1 - (\frac{\omega_\alpha}{\omega})^2] + M_{\alpha r} + iM_{\alpha i}\}\alpha_o = 0 \qquad (38)$$

where the subscripts r and i refer to the real and imaginary parts, respectively, of the coefficients. These are the equations that the unknowns h_o, α_o, U and ω must satisfy.

For a nontrivial solution for h_o and α_o, the determinant of (38) must vanish. Setting the determinant equal to zero yields two equations in μ and $(\omega_\alpha/\omega)^2$:

$$\frac{1}{\mu} = H\left(\frac{\omega_\alpha}{\omega}\right)^2 + J \tag{39}$$

and

$$\left(\frac{\omega_\alpha}{\omega}\right)^4 \{r_\alpha^2\left(\frac{\omega_h}{\omega_\alpha}\right)^2 - H[\left(\frac{\omega_h}{\omega_\alpha}\right)^2 M_{\alpha r} + r_\alpha^2 L_{hr}] + eH^2\}$$

$$-\left(\frac{\omega_\alpha}{\omega}\right)^2 \{r_\alpha^2[1 + \left(\frac{\omega_h}{\omega_\alpha}\right)^2] + J[\left(\frac{\omega_h}{\omega_\alpha}\right)^2 M_{\alpha r} + r_\alpha^2 L_{hr}]$$

$$-H[M_{\alpha r} + r_\alpha^2 L_{hr} - \beta x_\alpha \ell] - 2HJe\} \tag{40}$$

$$+ r_\alpha^2 - (\beta x_\alpha)^2 + J[M_{\alpha r} + r_\alpha^2 L_{hr} - \beta x_\alpha \ell] + eJ^2 = 0$$

where

$$d = L_{hr}M_{\alpha i} + L_{hi}M_{\alpha r} - L_{\alpha r}M_{hi} - L_{\alpha i}M_{hr}$$

$$e = L_{hr}M_{\alpha r} - L_{hi}M_{\alpha i} - L_{\alpha r}M_{hr} + L_{\alpha i}M_{hi}$$

$$f = L_{\alpha i} + M_{hi}$$

$$\ell = L_{\alpha r} + M_{hr}$$

$$H = \frac{1}{d}\left[\left(\frac{\omega_h}{\omega_\alpha}\right)^2 M_{\alpha i} + r_\alpha^2 L_{hi}\right]$$

$$J = \frac{-1}{d}\left[M_{\alpha i} + r_\alpha^2 L_{hi} - \beta x_\alpha f\right]$$

Eq. (40) is solved for $(\omega_\alpha/\omega)^2$ at chosen values of k and then μ is determined from (39). Finally, the flutter speed is evaluated from

$$\frac{U}{b\omega_\alpha} \equiv \frac{1}{k\left(\frac{\omega_\alpha}{\omega}\right)} \tag{41}$$

The hydrodynamic coefficients in heaving and pitching motion, as obtained by lifting surface theory with and without corrections for the leading edge singularity are presented in Tables IIIa and IIIb for the two foils at various k. Characteristic properties of these test models, as reported in Reference 5, are

Model	AR	x_α	r_α^2	ω_h/ω_α	β
1	4	0.195	0.573	0.533	1
2	2	0.167	0.571	0.533	1

These are the input to the flutter equations (39-41).

The results of these calculations by lifting surface theory are exhibited in Figure 18(A and B) where they are compared with the results of the two-dimensional approach and experiments. It is seen that flutter-speed predictions are non-conservative when hydrodynamic information is obtained by the uncorrected two-dimensional theory[29] or by the uncorrected three-dimensional theory, the two-dimensional approach yielding the less non-conservative predictions except in the very low density-ratio range. The poorest predictions are obtained by using hydrodynamic coefficients calculated by lifting surface theory with corrections for leading-edge singularity introduced after the solution of the integral equation. When use is made of the hydrodynamic coefficients obtained by lifting surface theory with corrections for leading-edge singularity before the inversion, the predictions are conservative throughout the density-ratio range. In fact, they are over-conservative by 10 to 30%.

The uncorrected lifting surface theory has been demonstrated to furnish hydrodynamic coefficients in best agreement with experiments. Yet these coefficients do not result in the best flutter speed predictions. This failure revives previous speculations. Is the proper mechanical and dynamical model being used to represent the stage of hydroelastic instability? Do the basic assumptions of lifting surface theory hold true at this stage (i.e., Kutta condition, leading-edge singularity, non-cavitating foil)? When hydrodynamic forces and moments are obtained by modifying the required chordwise mode shapes of the lifting surface theory, conservative flutter speed predictions result. The idea of modification of some basic assumptions of the lifting surface theory must be exploited further.

An attempt has been made to study the effect of structural damping[29] on the over-conservative flutter speed predictions obtained when the leading edge singularity is removed before the inversion of the integral equa-

tions. Figure 19(A and B) shows that, for increasing damping coefficients g from 0.01 to 0.10, the theoretical boundary for hydroelastic instability is brought closer and closer to the experimental values.

All of these results must be examined critically. No generalization can be made of the correctness of the mathematical model at this early stage.

CONCLUSIONS

This study includes a brief review of the unsteady lifting surface theory for a wing and of the technique of inverting the "downwash" integral equation by means of the "generalized lift operator" used in conjunction with the collocation method.

Expressions have been derived for the incident velocity distributions on a fully-submerged wing resulting from various modes of motion and ambient flow conditions: a) a wing moving in a sinusoidal gust, b) executing heaving motion, c) pitching about an arbitrary pivot point, and d) moving forward in a regular wave train. In addition, it is demonstrated that a surface-piercing vertical strut moving forward at high speed in regular waves or executing any mode of motion can be studied by treating a hydrodynamically equivalent wing of twice the aspect ratio with incident velocity distribution extended antisymmetrically with respect to the free surface at which level the incident velocity is zero. As a by-product of the present investigation, the traveling gust problem has been solved by the "generalized lift operator" approach and results are shown to coincide with the known explicit solution in two-dimensional flow conditions.

Systematic calculations have been performed for the main foil of the AG(EH) hydrofoil configuration, for which a detailed experimental study by O'Neill[11] is available, and for the simpler rectangular foils tested by Henry[12]. Unfortunately, the experiments of O'Neill were conducted on the foil attached to a long spheroidal pod whose presence could not be taken into account in the calculations. The calculated forces and moments for the AG(EH) main foil in pitching motion and in regular head seas show sizable discrepancies when compared to the experimental results, especially at low reduced frequencies where wing-pod interaction effects are most pronounced. Since the calculations for the foils of Ref. 12, without pods, agree well with the experimental results, the discrepancies in the case of the AG(EH) foil are realistic and must be attributed to the presence of the pod in the experiments. It should be emphasized that an accurate prediction of the hydrodynamic characteristics of a hydrofoil

with sizable pod is not possible unless a theoretical procedure is developed for taking into account the wing-pod interaction.

Removal of the physically unrealizable leading-edge singularity in the Birnbaum chordwise loading distribution by using the method of VanDyke and Lighthill before inverting the integral equation yields results inconsistent with experimental trends. On the other hand, when the singularity is removed after the inversion, the hydrodynamic forces and moments obtained are very close to the results without correction, with the advantage that a finite pressure is secured at the leading edge. The closeness of results with and without correction depends on the magnitude of the leading-edge radius. If the section is thick, the linearized correction formula is valid only in close proximity to the leading edge and should not be used to evaluate the lifting property of the section but only to obtain the finite pressure at the leading edge which is required for cavitation and fatigue studies.

Hydroelastic instability has been studied in the case of foils with two degrees of freedom, heave and pitch, using the two-dimensional theoretical hydrodynamic forces and moments and using the three-dimensional calculations with and without correction for the leading-edge singularity. In all cases but one, the common experience of non-conservative flutter speed predictions is repeated. However, when use is made of the hydrodynamic forces and moments obtained from the three-dimensional mathematical model where the leading-edge singularity is removed from the chordwise mode shapes before the inversion of the integral equation, the resulting flutter speed prediction is conservative. It is plausible that, at the stage of hydroelastic instability, there exists a chordwise loading distribution different from that required in the linear lifting surface theory. It could very well be that the modified distribution can be achieved by relaxing the Kutta condition as well as by removing the leading-edge singularity, or both. All these possibilities must be properly examined.

Although the introduction of structural damping brings the over-conservative boundary for hydroelastic instability close to the experimental boundary, this result must also be viewed with caution.

ACKNOWLEDGMENT

The authors wish to express their indebtedness to Dr. Charles J. Henry for his valuable discussions during the present investigation.

REFERENCES

1. *Henry, C.J.: "Hydrofoil Flutter Phenomenon and Airfoil Flutter Theory: 1 Density Ratio" DL Report 856, Stevens Institute of Technology, September 1961*

2. *Henry, C.J. and Ali, M.R.: "Hydrofoil Flutter Phenomenon and Airfoil Flutter Theory: II Center of Gravity Location" DL Report 911, SIT, July 1962*

3. *Henry, C.J. and Ali, M.R.: "Surface-Piercing Hydrofoil Flutter" DL Report 992, SIT, November 1963*

4. *Henry, C.J. and Ali, M.R.: "Hydrofoil Flutter Phenomenon and Airfoil Flutter Theory: III Sweep and Taper" DL Report 1115, SIT, December 1965.*

5. *Henry, C.J. and Ali, M.R.: "Hydrofoil Flutter Phenomenon and Airfoil Flutter Theory: IV Finite Aspect Ratio" DL Report 1170, SIT, October 1966*

6. *Rowe, W.S. and Marvin, T.G.: "A Program of Theoretical Research on Hydroelastic Stability" Final Report D6-19294, November 1968*

7. *Yates, E.C.: "Modified-Strip-Analysis Method for Predicting Wing Flutter at Subsonic to Hypersonic Speeds" AIAA, Jour. Aircraft, Vol. 3, No. 1, 1966*

8. *Yates, E.C.: "Flutter Prediction at Low Mass-Density Ratios with Application to the Finite-Span Noncavitating Hydrofoil" Third Marine Systems and ASW Meeting, May 1968*

9. *Chu, W.H. and Abramson, N.H.: "Further Calculations of the Flutter Speed of a Fully Submerged Subcavitating Hydrofoil" Tech. Report Contract No. N00014-68-C-0259, SWRI Proj. 02-2311, June 1968*

10. *Liu, Yuan-Ning and Besch, Peter K.: "Hydrofoil Flutter Analysis, Using a Modified Strip Theory" NSRDC Report No. 3624, July 1971*

11. *O'Neill, W.C.: "Unsteady Lift and Hinge Moment Characteristics of the AG(EH) Main Foil and Strut Assembly" NSRDC Report 2085, July 1968*

12. *Tsakonas, S. and Henry, C.J.: "Finite Aspect Ratio Hydrofoil Configurations in a Free Surface Wave System" DL Report 1118, Stevens Institute of Technology, July 1966*

13. Ashley, H. and Landahl, M.: Aerodynamics of Wings and Bodies. Addison-Wesley Publishing Co., Inc., Reading, Mass., 1965

14. Diehl, W.S.: Engineering Aerodynamics. Rev. Ed., Ronald Press, New York 1928

15. Bisplinghoff, R.L., Ashley, H. and Halfman, R.L.: Aeroelasticity. Addison-Wesley Publishing Co., Inc., Reading, Mass. 1955

16. Engineering Sciences Data, Item No. 70011, Aeronautical Series, Royal Aeronautical Society, 1970

17. Van Dyke, M.D.: "Second-Order Subsonic Airfoil Theory Including Edge Effects" NACA Report 1274, 1956

18. Lighthill, M.J.: "A New Approach to Thin Aerofoil Theory" Aero Quart., Vol. 3, pt. 3, November 1951, pp. 193-210

19. Jacobs, W.R. and Tsakonas, S.: "A New Procedure for the Solution of Lifting-Surface Problems" Jour. of Hydronautics, Vol. 3, No. 1, January 1969

20. Tsakonas, S., Jacobs, W.R. and Ali, M.R.: "A Theory for the Propeller-Rudder Interaction" Report SIT-DL-68-1284, Stevens Institute of Technology, August 1968; published as "Application of the Unsteady-Lifting-Surface Theory to the Study of Propeller-Rudder Interaction" Jour. Ship Research, Vol. 14, No. 3, September 1970, pp. 181-194

21. Jones, R.T. and Cohen, D.: "High Speed Wing Theory" Princeton Aeronautical Paperbacks No. 6, Princeton University Press, Princeton, N.J. 1960

22. Falkner, V.M.: "Calculated Loadings Due to Incidence of a Number of Straight and Swept-back Wings" R&M 2596, 1948, Aeronautical Research Council

23. Kemp, N.H.: "On the Lift and Circulation of Airfoils in Some Unsteady Flow Problems" Jour. Aeronautical Sciences, Oct. 1952

24. Reissner, E. and Stevens, J.: "Effects of Finite Span on the Airload Distributions for Oscillating Wing. II - Methods of Calculation and Examples of Application" NACA TN 1195, 1947

25. Leehey, Patrick: "The Hilbert Problem for an Airfoil in Unsteady Flow" DTMB Report 1077, January 1957

26. Kaplan, P.: "A Hydrodynamic Theory for the Forces on Hydrofoils in Unsteady Motion" Stevens Institute of Technology Dissertation, 1955

27. Havelock, T.H.: "The Forces on a Submerged Body Moving Under Waves" Transactions of the Institution of Naval Architects, January 1954

28. *Landahl, M.: "Pressure-Loading Functions for Oscillating Wings with Control Surfaces" AIAA Vol. 6, No. 2, February 1968*

29. *Scanlan, R.H. and Rosenbaum, R.: Introduction to the Study of Aircraft Vibration and Flutter, The MacMillan Co., N.Y., 1951*

30. *Magnus, W. and Oberbettinger, F.: Formulas and Theorems for the Functions of Mathematical Physics, Chelsea Publishing Co., New York, N.Y., 1954*

31. *McLachlan, N.W.: Bessel Functions for Engineers. Second edition, Oxford University Press, London, England, 1961*

TABLE Ia

AG(EH) MAIN FOIL IN PITCHING MOTION

Unsteady Lift Curve Slopes with and without Correction for Leading-Edge Singularity

A) Pivot point at 0.062c

$k' = \frac{\omega c_o}{U}$	$k = \frac{\omega b}{U}$	Unsteady Lift Curve Slope C_{L_α} Without correction		Correction for l.e. singularity before solution		Correction for l.e. singularity after solution	
		Mag.	Phase	Mag.	Phase	Mag.	Phase
0	0	3.650	0°	4.132	0°	3.326	0°
.05	.0325	3.641	2.3	4.119	1.8	3.317	2.6
.10	.065	3.624	5.1	4.094	4.0	3.303	5.6
.45	.293	3.664	26.4	4.009	22.5	3.391	28.8
.60	.390	3.826	36.0	4.101	31.4	3.579	38.8
1.10	.715	4.914	62.2	4.982	57.9	4.751	65.3
1.40	.910	5.845	73.4	5.823	69.9	5.722	76.3
1.70	1.105	6.900	82.6	6.808	79.7		
2.40	1.560	9.823	98.6	9.608	97.0	9.793	100.6
B) Pivot point at 0.32c							
0	0	3.650	0°	4.132	0°	3.326	0°
.05	.0325	3.639	1.4				
.10	.065	3.616	3.2	4.086	2.1	3.295	3.7
.45	.293	3.525	18.8	3.868	14.7	3.254	21.3
.60	.390			3.641	21.7	3.362	29.7
1.10	.715	4.372	48.8	4.403	43.7	4.234	52.4
1.40	.910	5.069	57.8	4.992	53.5	4.984	61.3
1.70	1.105	5.842	64.8	5.674	61.3		
2.40	1.560	7.810	75.9	7.478	74.0	7.857	78.6

c_o = half root chord

b = half geometric mean chord

$C_L = \frac{L}{\frac{1}{2}\rho U^2 S}$, S = area of foil

TABLE Ib

AG(EH) MAIN FOIL IN PITCHING MOTION

Unsteady Moment Curve Slopes with and without Correction for Leading-Edge Singularity

A) Pivot point at 0.062c

$k' = \frac{\omega c_o}{U}$	$k = \frac{\omega b}{U}$	Unsteady Moment Curve Slope C_{m_α} Without correction		Correction for l.e. singularity before solution		Correction for l.e. singularity after solution	
		Mag.	Phase	Mag.	Phase	Mag.	Phase
0	0	.582	0°	.462	0°	.535	0°
.05	.0325	.583	6.5	.463	8.3	.536	7.1
.10	.065	.587	13.5	.471	17.0	.542	14.5
.45	.293	.792	55.8	.736	64.0	.760	58.2
.60	.390	.956	68.1	.927	75.6	.928	70.3
1.10	.715	1.674	92.6	1.712	96.8	1.648	94.1
1.40	.910	2.187	101.6	2.256	104.5	2.160	102.8
1.70	1.105	2.754	108.9	2.842	110.9		
2.40	1.560	4.325	121.8	4.444	122.5	4.285	122.7

B) Pivot point at 0.32c

0	0	.359	180°	.603	180°	.322	180°
.05	.0325	.360	174.6				
.10	.065	.365	169.6	.607	172.1	.329	169.0°
.45	.293	.484	143.8	.712	150.4	.446	142.6
.60	.390			.794	144.6	.527	137.3
1.10	.715	.911	132.2	1.155	135.2	.860	131.7
1.40	.910	1.161	132.3	1.421	133.6	1.100	132.1
1.70	1.105	1.435	133.7	1.710	133.5		
2.40	1.560	2.195	138.4	2.498	136.1	2.101	139.0

$$C_m = \frac{L}{\frac{1}{2}\rho U^2 Sb}$$

TABLE IIa

AG(EH) IN HEAD SEAS

Lift and Hinge Moment Coefficients

A) U = 14.2 kts. = 23.98 ft/sec.

				Pivot point →		0.062c				0.32c	
$k' = \frac{\omega c_o}{U}$	$k = \frac{\omega b}{U}$	λ/c_o	λ/c	$C_L \frac{b}{a}$		$C_H \frac{b}{a}$		$C_L \frac{b}{a}$		$C_H \frac{b}{a}$	
				Mag.	*Phase*	*Mag.*	*Phase*	*Mag.*	*Phase*	*Mag.*	*Phase*
.10	.065	108.9	83.8	.0909	-92.6°	.0144	-94.3°	.0908	-91.5°	.0090	+91.3°
.17	.110	56.5	43.5	.1142	-94.6	.0182	-98.2	.1142	-92.4	.0113	93.5
.27	.175	32.6	25.1	.1284	-97.1	.0206	-103.8	.1284	-93.4	.0129	97.6
.40	.260	20.7	16.0	.1294	-99.8	.0210	-110.7	.1294	-93.9	.0134	103.4
.60	.390	13.1	10.1	.1144	-102.2	.0191	-119.8	.1145	-93.0	.0126	114.3
.85	.552	8.9	6.9	.0889	-103.1	.0158	-128.8	.0889	-89.7	.0110	128.7
1.15	.747	6.4	5.0	.0614	-103.1	.0120	-137.0	.0614	-84.4	.0090	144.5

B) U = 20.5 kts. = 34.62 ft/sec.

.10	.065	92.2	71.0	.0673	-93.1°	.0107	-95.3°	.0673	-91.9°	.0066	+91.7°
.17	.110	49.6	38.2	.0825	-95.4	.0132	-100.0	.0824	-92.9	.0082	94.9
.27	.175	29.4	22.6	.0906	-98.1	.0146	-106.3	.0906	-94.0	.0091	98.8
.40	.260	19.0	14.7	.0895	-101.2	.0146	-113.7	.0895	-94.8	.0093	105.5
.60	.390	12.3	9.4	.0774	-103.9	.0132	-124.2	.0774	-94.8	.0087	116.6
.85	.552	8.4	6.5	.0587	-105.3	.0107	-133.8	.0586	-91.0	.0077	130.8
1.15	.747	6.1	4.7	.0395	-105.6	.0081	-143.0	.0394	-85.9	.0062	146.8

TABLE IIb

AG(EH) IN HEAD SEAS

Lift and Hinge Moment Coefficients
with Correction for Leading-Edge Singularity Before Solution

A) U = 14.2 kts. = 23.98 ft/sec.

				Pivot point →		0.062c				0.32c	
$k' = \frac{\omega c_o}{U}$	$k = \frac{\omega b}{U}$	λ/c_o	λ/c	$C_L \frac{b}{a}$		$C_H \frac{b}{a}$		$C_L \frac{b}{a}$		$C_H \frac{b}{a}$	
				Mag.	*Phase*	*Mag.*	*Phase*	*Mag.*	*Phase*	*Mag.*	*Phase*
.10	.065	108.9	83.5	.1027	-92.9°	.0115	-95.7°	.1027	-91.8°	.0151	+90.3°
.27	.175	32.6	25.1	.1449	-97.7	.0163	-108.6	.1449	-94.0	.0216	94.2
.40	.260	20.7	16.0	.1459	-100.6	.0169	-118.0	.1459	-94.7	.0221	98.4
.60	.390	13.1	10.1	.1288	-103.2	.0159	-130.3	.1288	-94.0	.0204	106.6
1.15	.747	6.4	5.0	.0689	-104.5	.0112	-152.1				
				B) U = 20.5 kts. = 34.62 ft/sec.							
.10	.065	92.2	71.0	.0761	-93.4°	.0085	-97.2°	.0761	-92.1	.0112	+90.8°
.27	.175	29.4	22.6	.1023	-98.6	.0117	-111.6	.1023	-94.5	.0153	95.4
.40	.260	19.0	14.7	.1010	-101.8	.0119	-121.8	.1010	-95.4	.0154	100.0
.60	.390	12.3	9.4	.0871	-104.8	.0111	-134.9	.0871	-94.9	.0140	108.7
1.15	.747	6.1	4.7	.0441	-106.8	.0077	-157.5	.0441	-87.1	.0088	135.7

TABLE IIc

AG(EH) IN HEAD SEAS

Lift and Hinge Moment Coefficients
with Correction for Leading-Edge Singularity After Solution

A) U = 14.2 kts. = 23.98 ft/sec.

		Pivot point →		0.062c				0.32c			
$k' = \frac{\omega c_o}{U}$	$k = \frac{\omega b}{U}$	λ/c_o	λ/c	$C_L \frac{b}{a}$		$C_H \frac{b}{a}$		$C_L \frac{b}{a}$		$C_H \frac{b}{a}$	
				Mag.	*Phase*	*Mag.*	*Phase*	*Mag.*	*Phase*	*Mag.*	*Phase*
.10	.065	108.9	83.5	.0827	-92.6°	.0133	-94.2°	.0827	-91.5°	.0081	+91.1°
.27	.175	32.6	25.1	.1168	-97.1	.0189	-103.6	.1168	-93.4	.0116	97.3
.40	.260	20.7	16.0	.1177	-99.8	.0192	-110.4	.1177	-94.0	.0120	103.2
.60	.390	13.1	10.1	.1041	-102.3	.0175	-119.4	.1041	-93.1	.0114	113.9
1.15	.747	6.4	5.0	.0559	-103.4	.0110	-136.9				

B) U = 20.5 kts. = 34.62 ft/sec.

.10	.065	92.2	71.0	.0613	-93.2°	.0099	-95.4°	.0613	-91.8°	.0060	+91.9°
.27	.175	29.4	22.6	.0825	-98.2	.0134	-106.1	.0825	-94.1	.0082	98.9
.40	.260	19.0	14.7	.0814	-101.2	.0135	-113.7	.0814	-94.9	.0084	105.4
.60	.390	12.3	9.4	.0704	-104.2	.0121	-123.7	.0704	-94.3	.0079	116.5
1.15	.747	6.1	4.7	.0359	-106.2	.0074	-142.9	.0359	-86.5	.0055	146.4

TABLE IIIa

HYDRODYNAMIC COEFFICIENTS FOR USE IN THREE-DIMENSIONAL FLUTTER ANALYSIS

Rectangular Foil of Aspect Ratio AR = 4 (Model 1)

A) Without correction for leading-edge singularity

k	$1/k$	L_h		M_h		L_α		M_α	
$\frac{b\omega}{U}$	$\frac{U}{b\omega}$	R	Im	R	Im	R	Im	R	Im
.10	10.00	-.1095	-12.233	.4619	.2705	-122.898	-11.231	3.077	-9.073
.15	6.67	.0657	-7.933	.4588	.1766	-53.283	-8.433	1.547	-6.032
.20	5.00	.1885	-5.785	.4567	.1283	-29.196	-6.772	1.009	-4.518
.25	4.00	.2799	-4.505	.4552	.0984	-18.200	-5.658	.7592	-3.613
.30	3.33	.3507	-3.663	.4541	.0780	-12.318	-4.857	.6240	-3.011
.35	2.86	.4074	-3.071	.4532	.0631	-8.827	-4.254	.5433	-2.582

B) With correction for leading-edge singularity after solution

.10	10.00	.0438	-9.880	.3847	-.7492	-99.181	-11.889	-7.207	-8.557
.15	6.67	.1860	-6.406	.3958	-.4854	-42.948	-8.693	-2.939	-5.766
.20	5.00	.2857	-4.671	.4037	-.3547	-23.494	-6.883	-1.469	-4.354
.25	4.00	.3601	-3.637	.4095	-.2778	-14.615	-5.703	-.8014	-3.500
.30	3.33	.4178	-2.957	.4140	-.2280	-9.865	-4.869	-.4456	-2.928
.35	2.86	.4641	-2.480	.4176	-.1934	-7.047	-4.249	-.2348	-2.518

C) With correction for leading-edge singularity before solution

.20	5.00	-.3845	-9.218	.6123	1.0592	-46.820	-4.543	5.784	-5.083
.25	4.00	-.2304	-7.166	.5938	.8138	-29.245	-4.043	3.745	-4.020
.30	3.33	-.1112	-5.815	.5793	.6592	-19.846	-3.609	2.653	-3.324
.35	2.86	-.0160	-4.866	.5675	.5463	-14.273	-3.245	2.005	-2.833
.40	2.50	.0630	-4.169	.5575	.4629	-10.713	-2.946	1.591	-2.468
.45	2.22	.1322	-3.638	.5488	.3997	-8.308	-2.703	1.314	-2.185
.50	2.00	.1986	-3.221	.5402	.3513	-6.600	-2.512	1.120	-1.957
.55	1.82	.2705	-2.883	.5306	.3146	-5.328	-2.372	.982	-1.765

TABLE IIIb

HYDRODYNAMIC COEFFICIENTS FOR USE IN THREE-DIMENSIONAL FLUTTER ANALYSIS

Rectangular Foil of Aspect Ratio AR = 2 (Model 2)

A) Without correction for leading-edge singularity

k	1/k	L_h		M_h		L_α		M_α	
$\frac{b\omega}{U}$	$\frac{U}{b\omega}$	R	Im	R	Im	R	Im	R	Im
.2	5.00	.5337	-4.282	.4003	.2340	-21.297	-7.122	1.5031	-3.959
.3	3.33	.5734	-2.791	.3987	.1513	-9.144	-4.812	.8358	-2.639
.4	2.50	.6026	-2.052	.3976	.1099	-4.938	-3.638	.6045	-1.981
.5	2.00	.6292	-1.614	.3963	.0859	-3.005	-2.934	.5002	-1.585
.6	1.67	.6582	-1.320	.3942	.0721	-1.946	-2.469	.4467	-1.317
.7	1.43	.6821	-1.112	.3925	.0626	-1.310	-..132	.4146	-1.126
.8	1.25	.7005	-.8959	.3915	.0552	-.9005	-1.874	.3932	-.9841
.9	1.11	.7147	-.8427	.3912	.0492	-.6241	-1.672	.3782	-.8747
1.0	1.00	.7260	-.7520	.3912	.0442	-.4284	-1.510	.3672	-.7877
B) With correction for leading-edge singularity after solution									
.2	5.00	.5528	-3.398	.3821	-.1544	-16.816	-7.009	-.4671	-3.905
.3	3.33	.5847	-2.215	.3838	-.1019	-7.175	-4.726	-.0335	-2.608
.4	2.50	.6084	-1.628	.3851	-.0765	-3.839	-3.569	.1163	-1.960
.5	2.00	.6298	-1.280	.3861	-.0609	-2.305	-2.874	.1867	-1.570
.6	1.67	.6529	-1.046	.3865	-.0485	-1.464	-2.414	.2285	-1.307
.7	1.43	.6719	-.8797	.3870	-.0395	-.9572	-2.080	.2537	-1.119
.8	1.25	.6866	-.7577	.3876	-.0332	-.6325	-1.828	.2693	-.9787
.9	1.11	.6982	-.6654	.3884	-.0288	-.4131	-1.630	.2793	-.8704
1.0	1.00	.7005	-.5933	.3893	-.0257	-.2580	-1.471	.2862	-.7841
C) With correction for leading-edge singularity before solution									
.20	5.00	.2667	-7.033	.4750	.9829	-35.226	-5.980	5.294	-4.245
.25	4.00	.3040	-5.558	.4695	.7743	-22.256	-4.863	3.471	-3.385
.30	3.33	.3346	-4.577	.4649	.6349	-15.248	-4.097	2.485	-2.815
.35	2.86	.3608	-3.879	.4609	.5354	-11.048	-3.540	1.895	-2.410
.40	2.50	.3844	-3.359	.4572	.4611	-8.338	-3.119	1.514	-2.106
.45	2.22	.4066	-2.957	.4536	.4037	-6.489	-2.791	1.255	-1.870
.50	2.00	.4295	-2.637	.4498	.3584	-5.168	-2.533	1.072	-1.679
.55	1.82	.4550	-2.374	.4453	.3224	-4.185	-2.327	.9369	-1.521

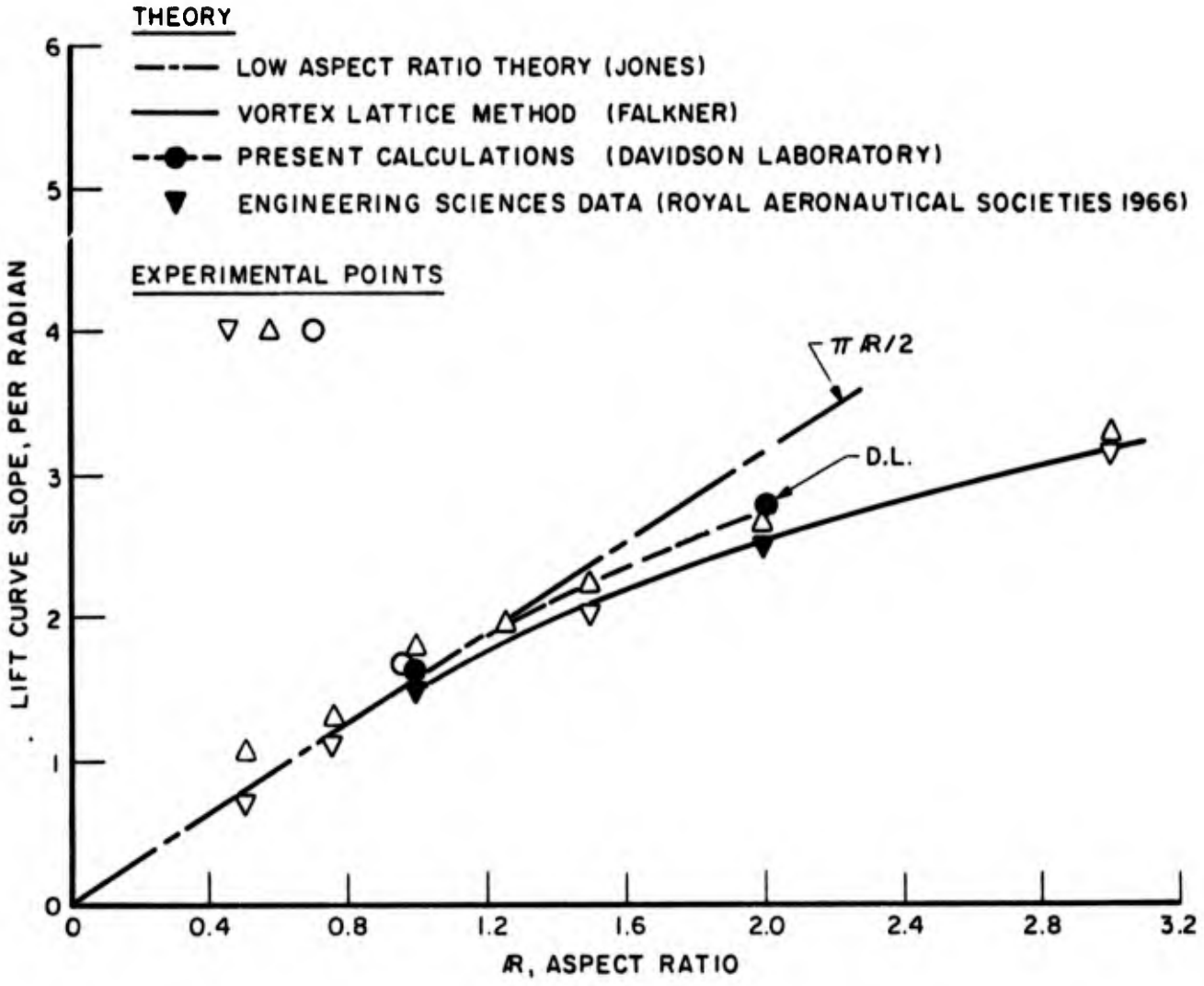

FIG. 1. COMPARISON OF EXPERIMENTAL AND THEORETICAL VALUES OF THE LIFT CURVE SLOPE FOR UNTAPERED WINGS OF 0° SWEEP (STEADY-STATE)

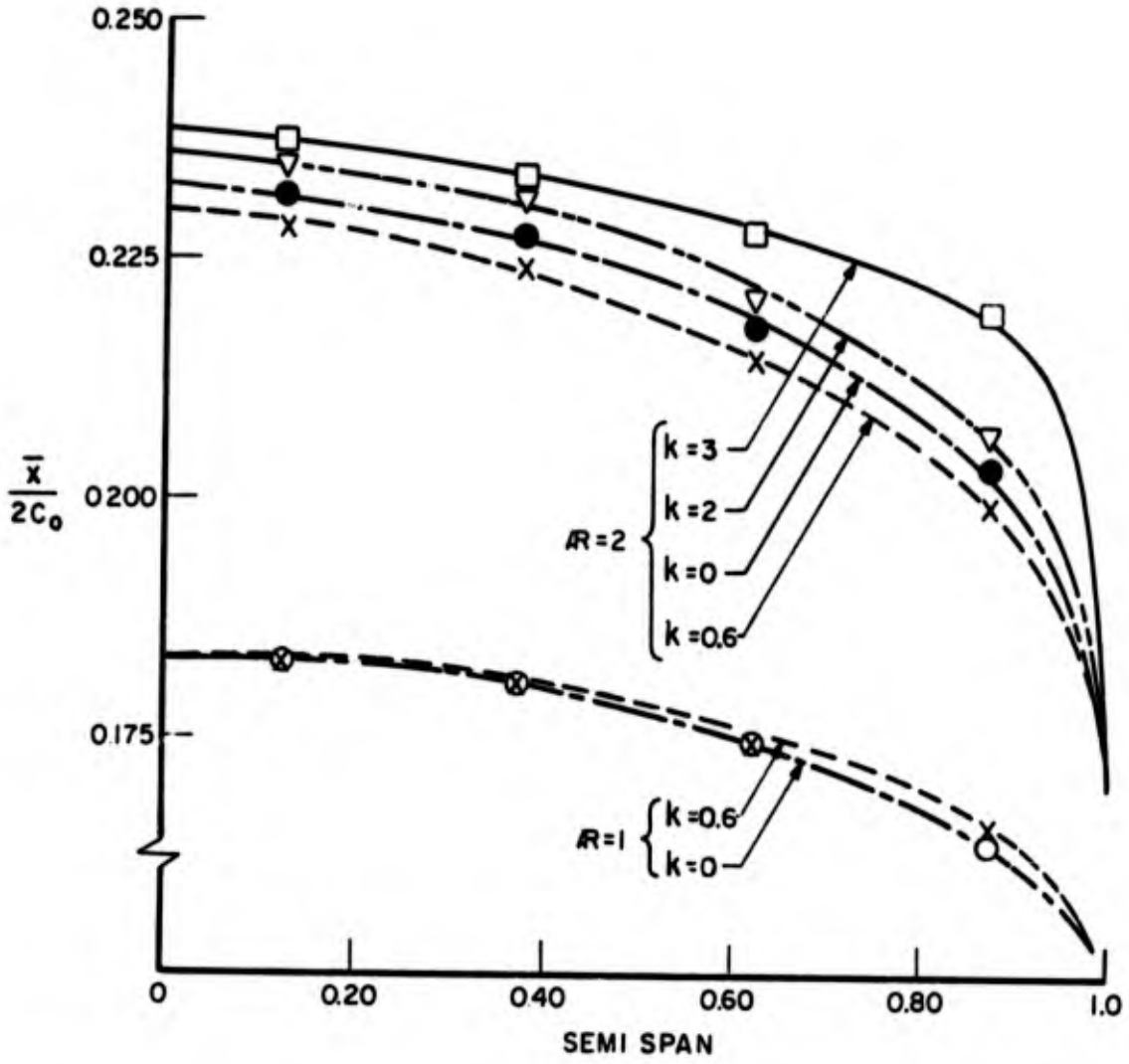

FIG. 2. LOCATIONS OF CENTER OF PRESSURE $\bar{x}/2C_0$ AFT OF LEADING EDGE

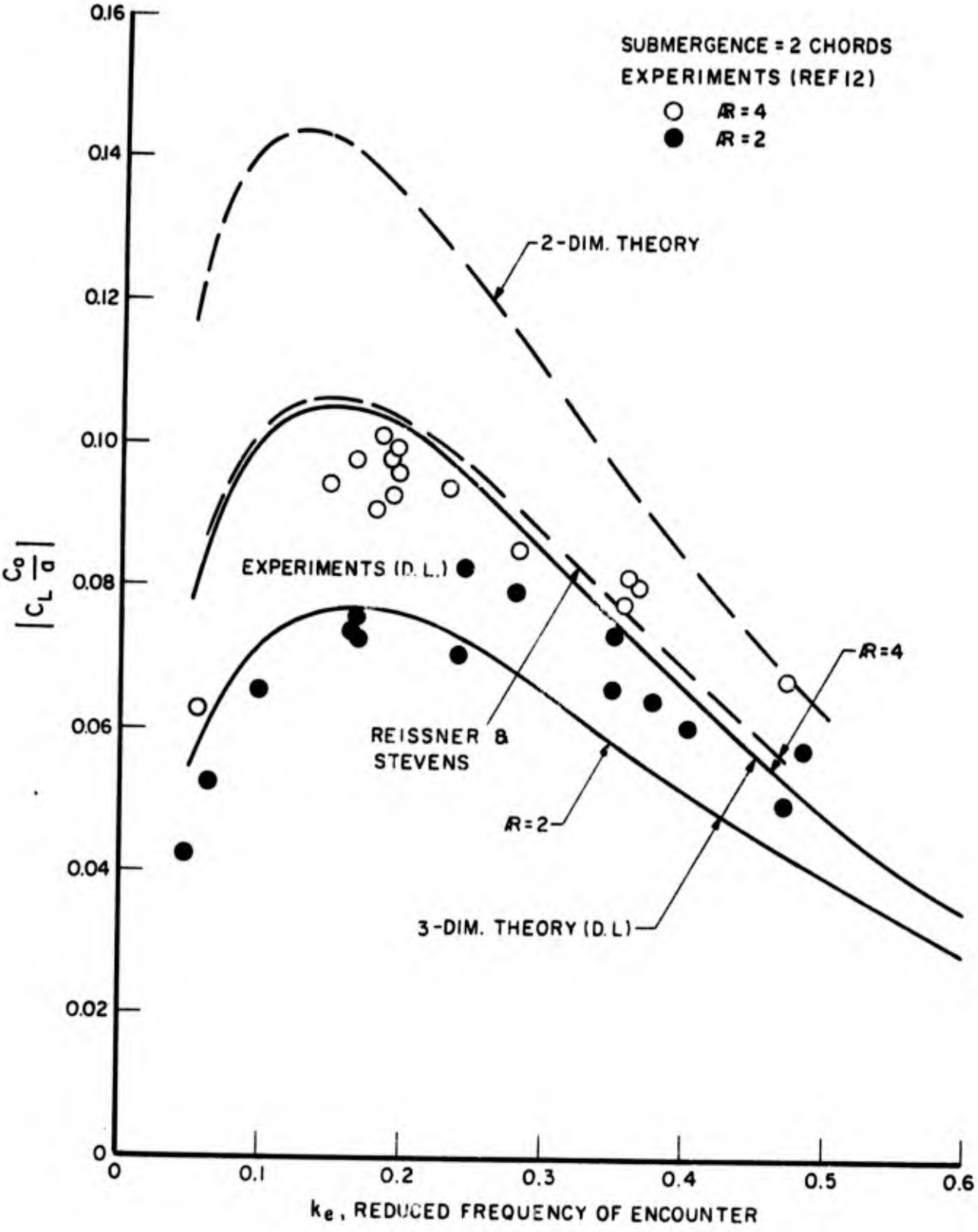

FIG. 3. LIFT RESPONSE COEFFICIENTS OF RECTANGULAR FOILS OF NACA 64-012 SECTION AT 15 f.p.s. IN REGULAR HEAD SEAS

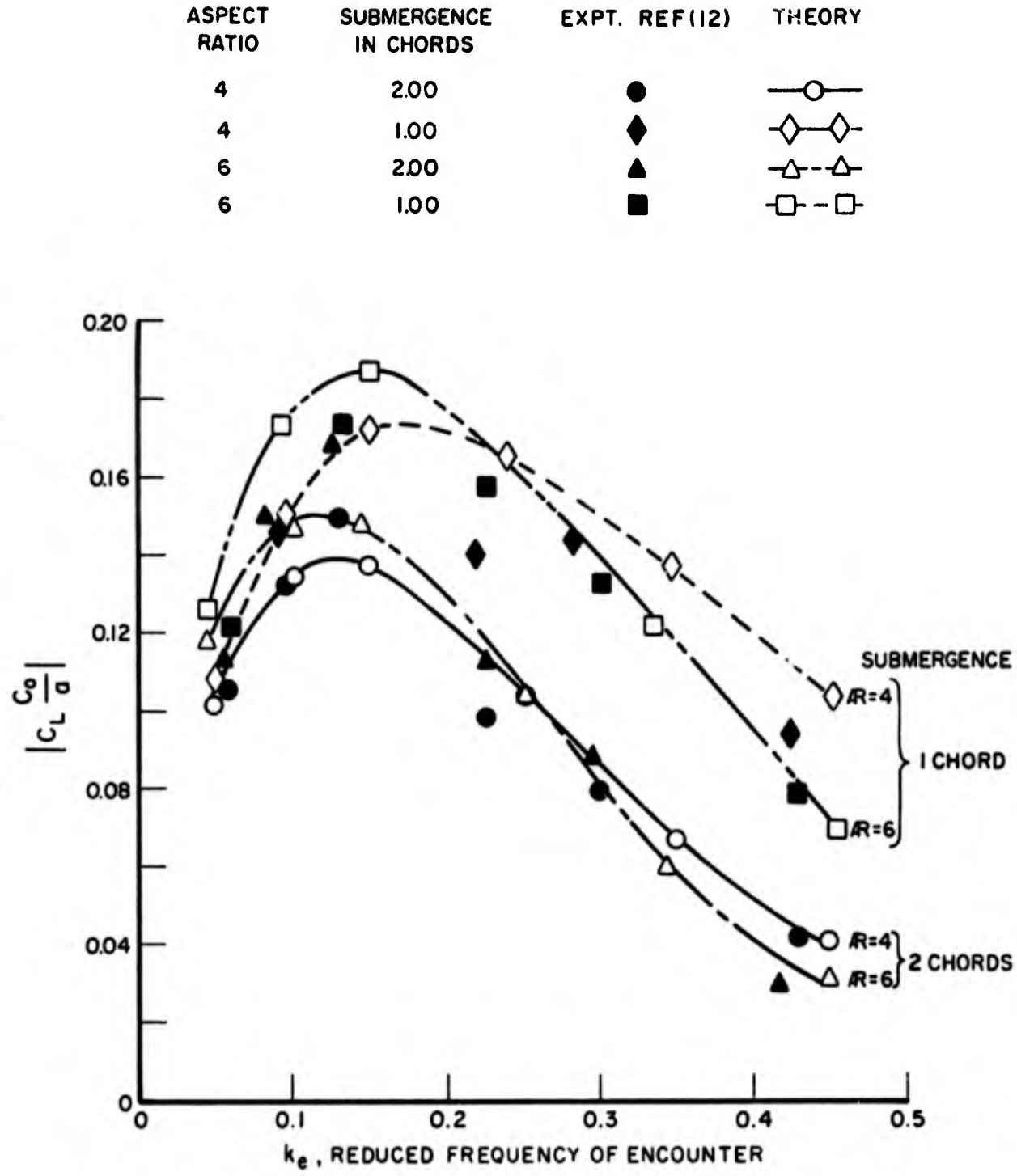

FIG. 4. LIFT RESPONSE COEFFICIENTS OF RECTANGULAR FOILS OF NACA 64-012 SECTION AT 11.9 fps IN REGULAR OBLIQUE SEAS (HEADING ANGLE $\gamma = 45°$)

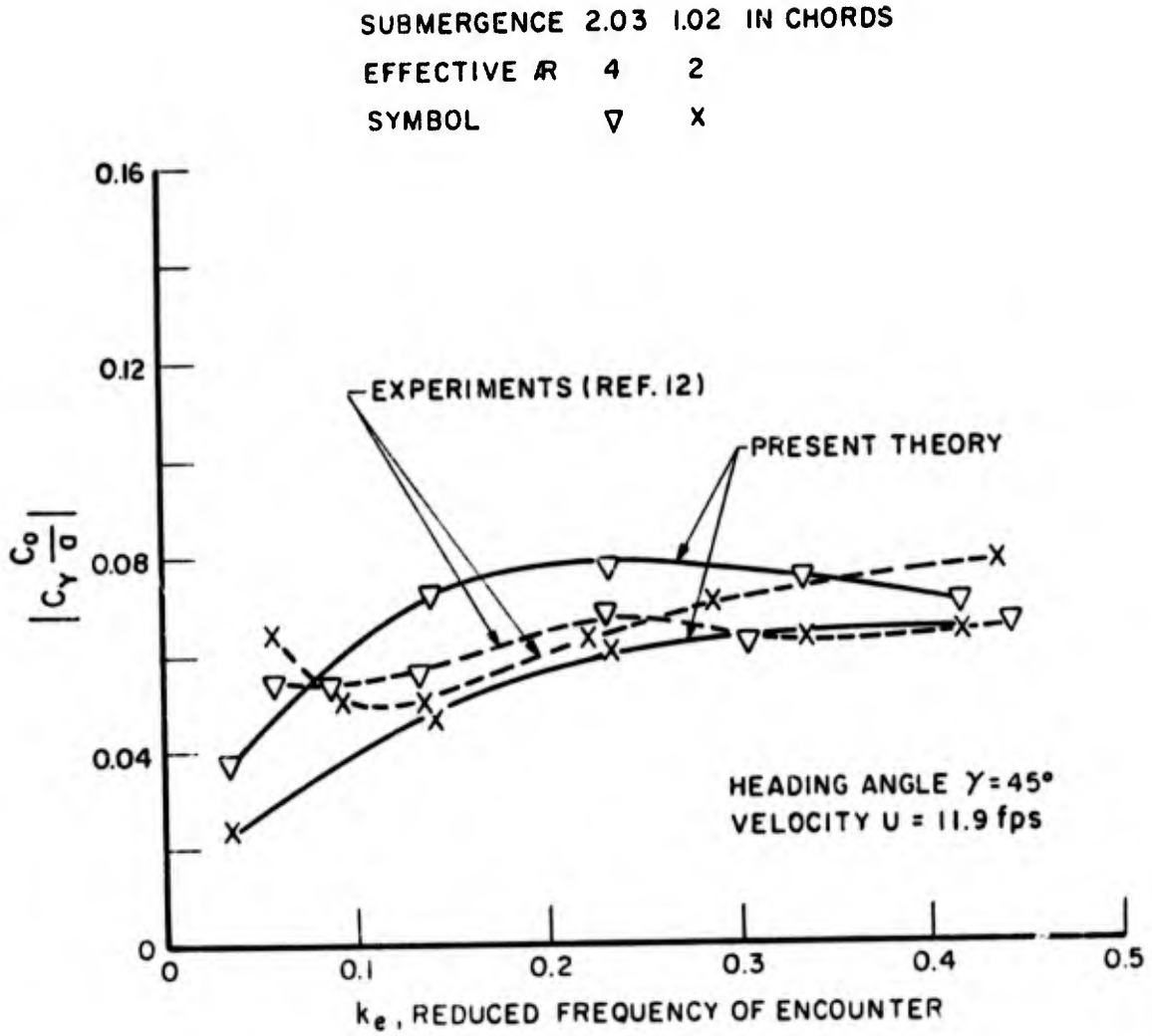

FIG. 5. SIDE FORCE RESPONSE COEFFICIENT FOR VERTICAL STRUT IN OBLIQUE WAVES

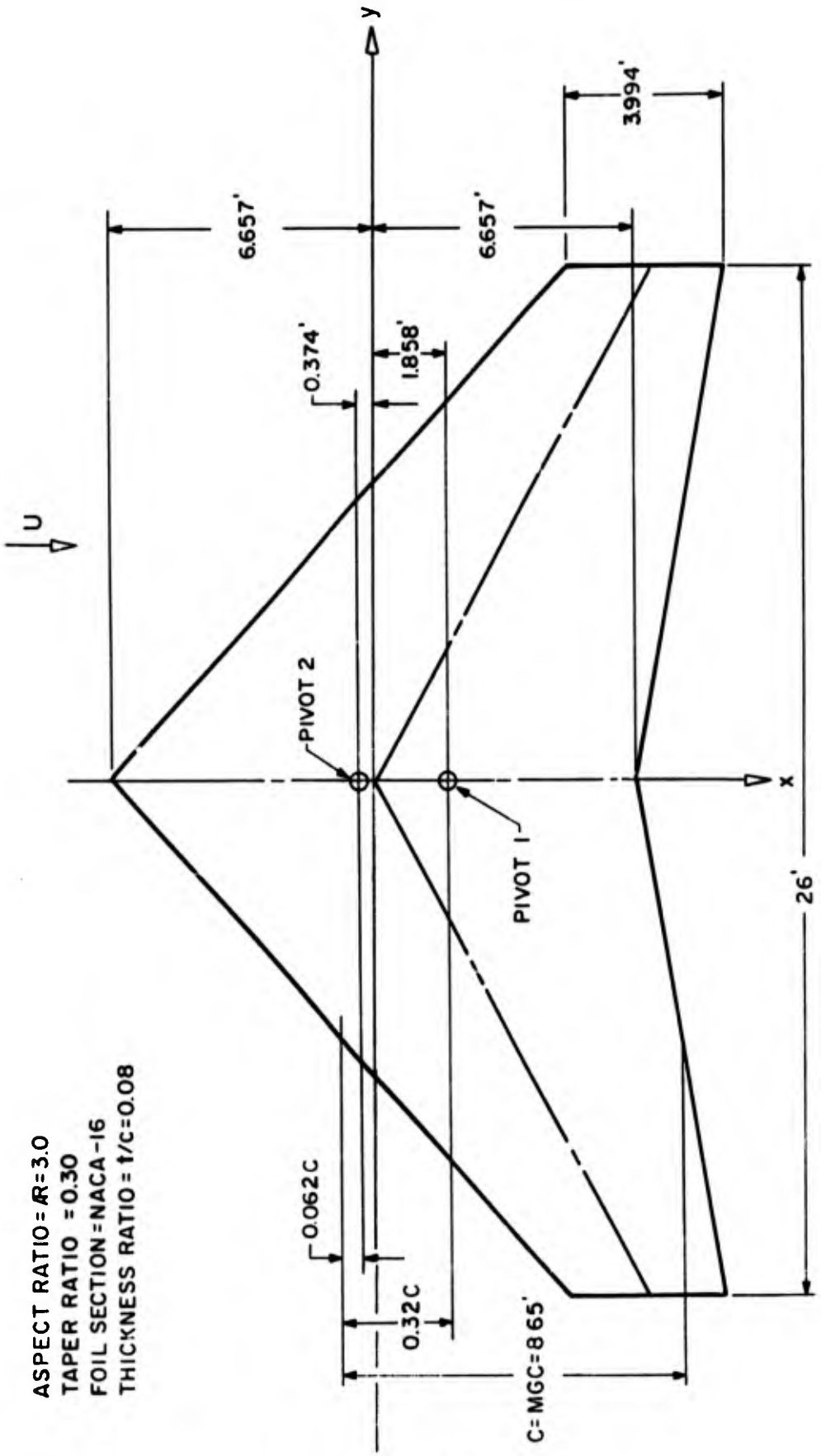

FIG. 6. PRINCIPAL DIMENSIONS OF AG (EH) MAIN FOIL

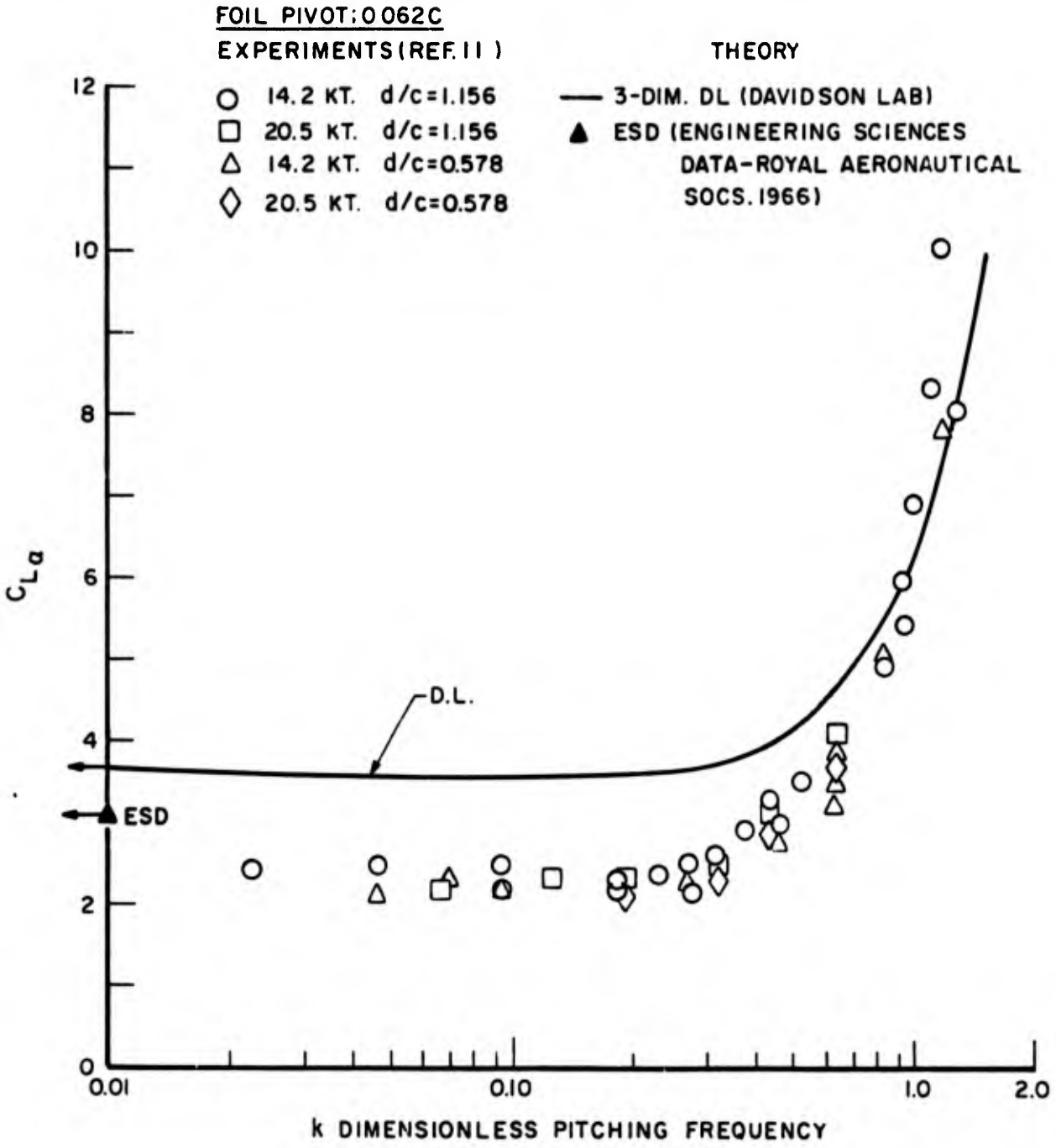

FIG. 7. UNSTEADY LIFT CURVE SLOPE OF THE MAIN FOIL OF AG (EH)

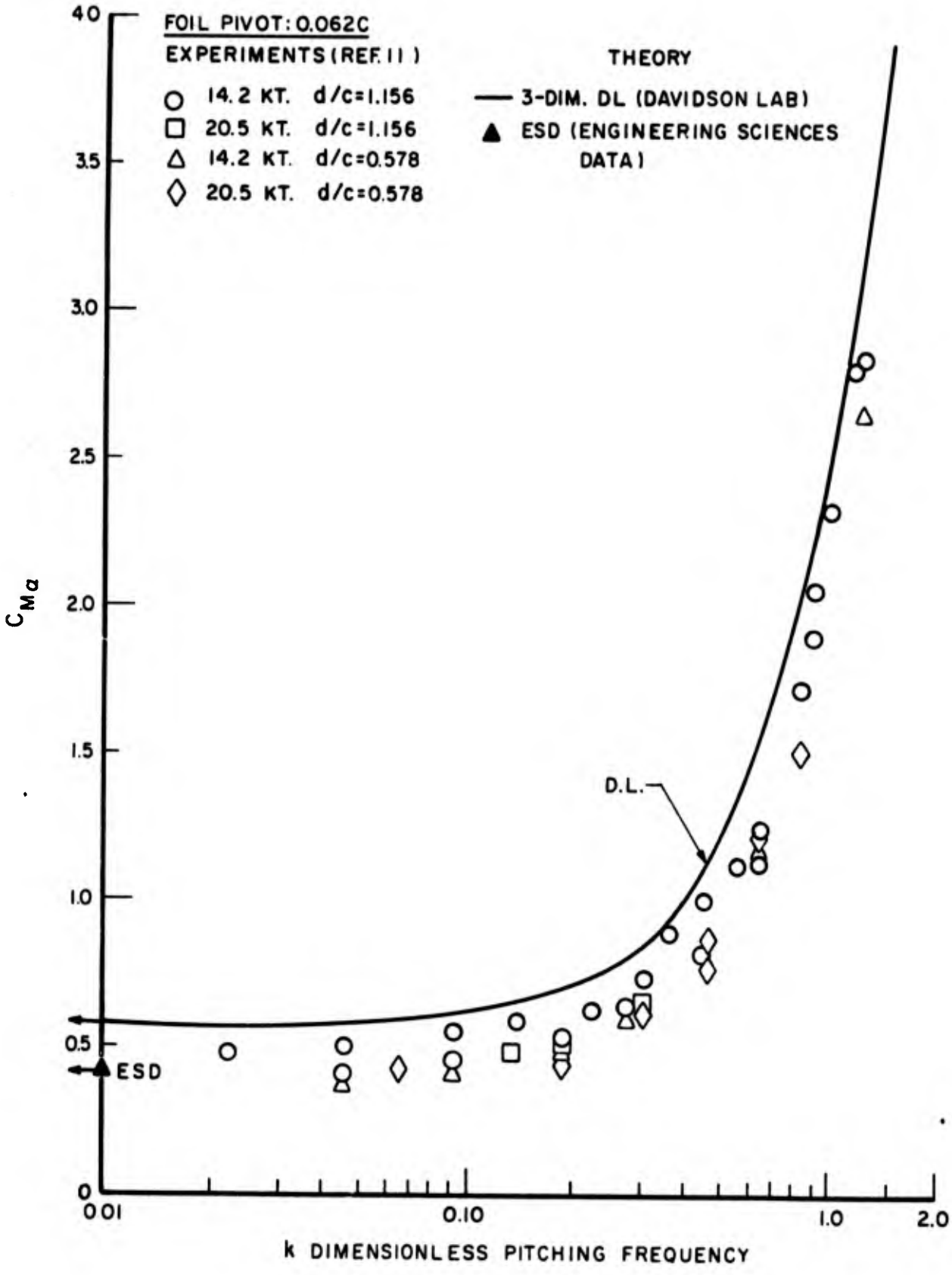

FIG 8. UNSTEADY MOMENT CURVE SLOPE OF THE MAIN FOIL OF AG(EH)

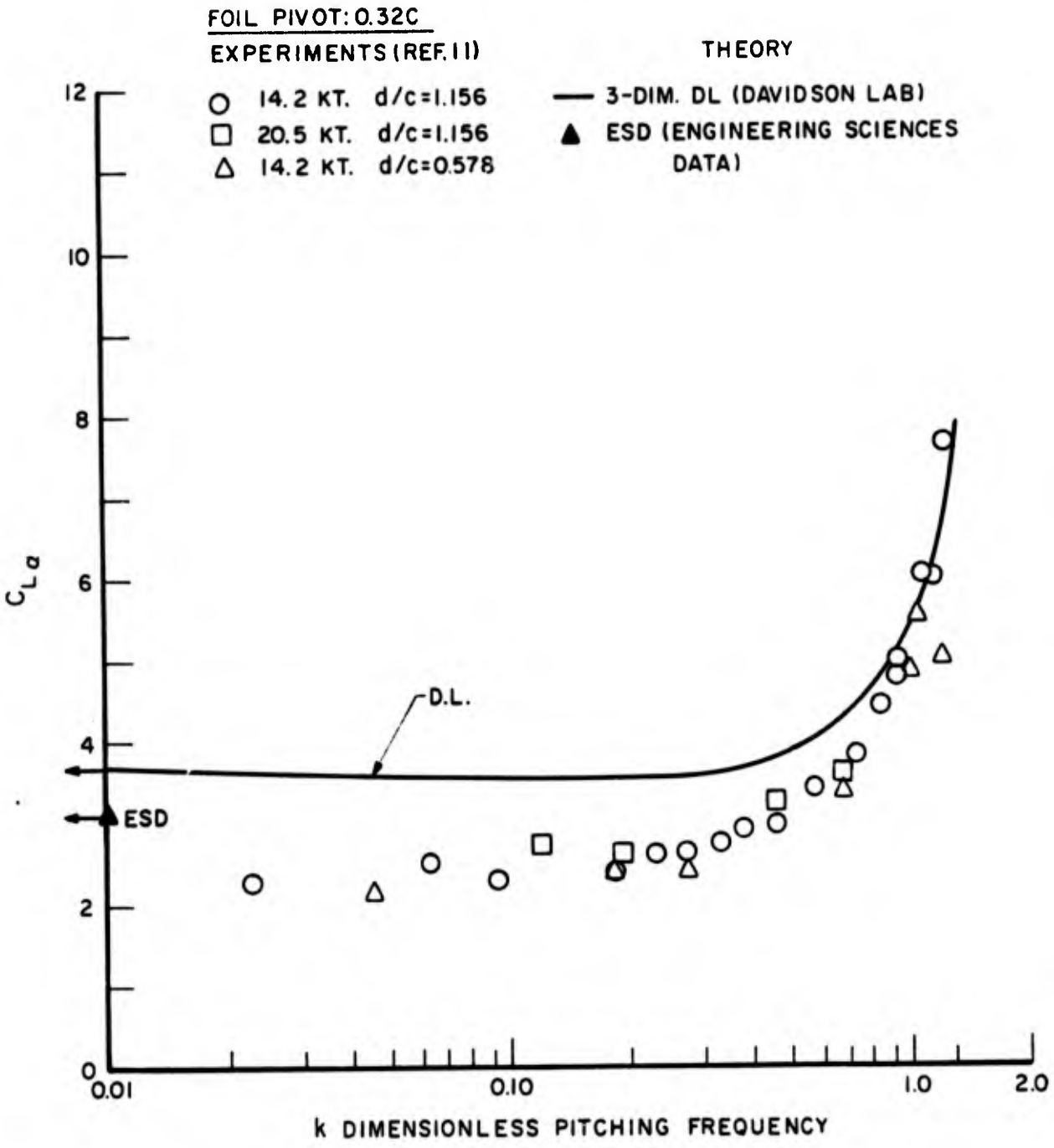

FIG. 9. UNSTEADY LIFT CURVE SLOPE OF THE MAIN FOIL OF AG (EH)

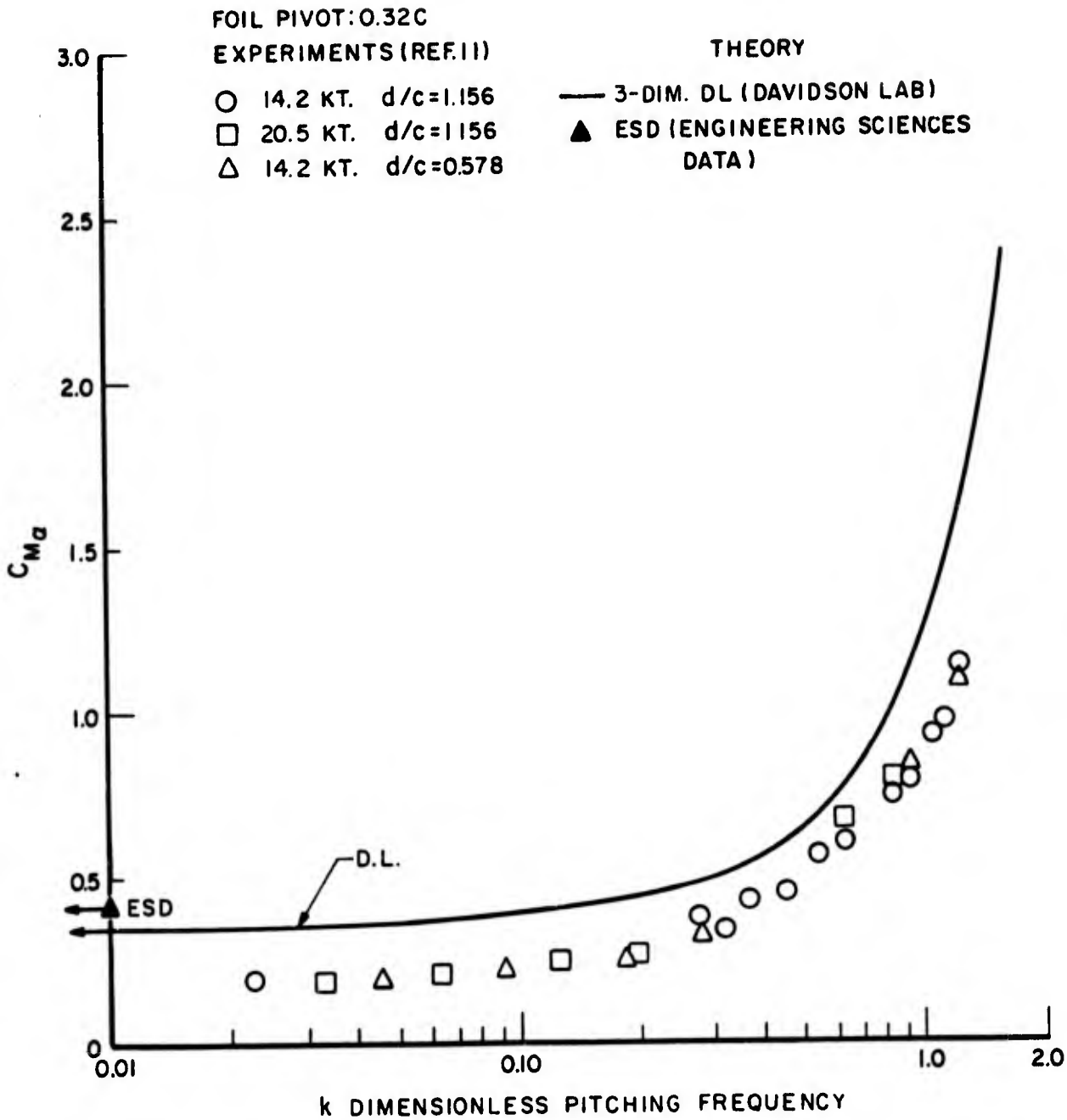

FIG. 10. UNSTEADY MOMENT CURVE SLOPE OF THE MAIN FOIL OF AG(EH)

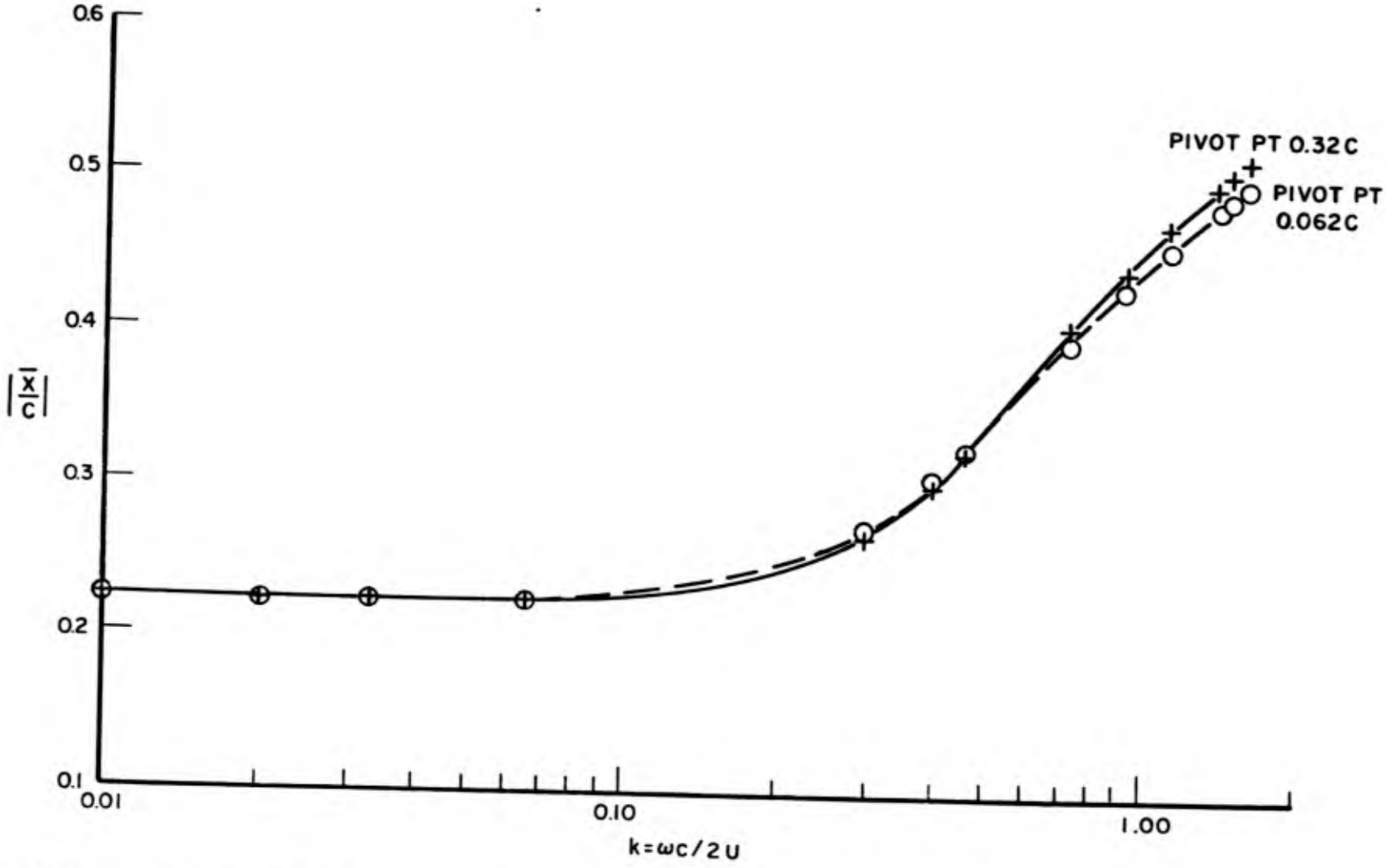

FIG. 11. LOCATION OF CENTER OF PRESSURES AFT OF LEADING EDGE OF MEAN GEOMETRIC CHORD FOR AG(EH) FOIL IN PITCHING MOTION

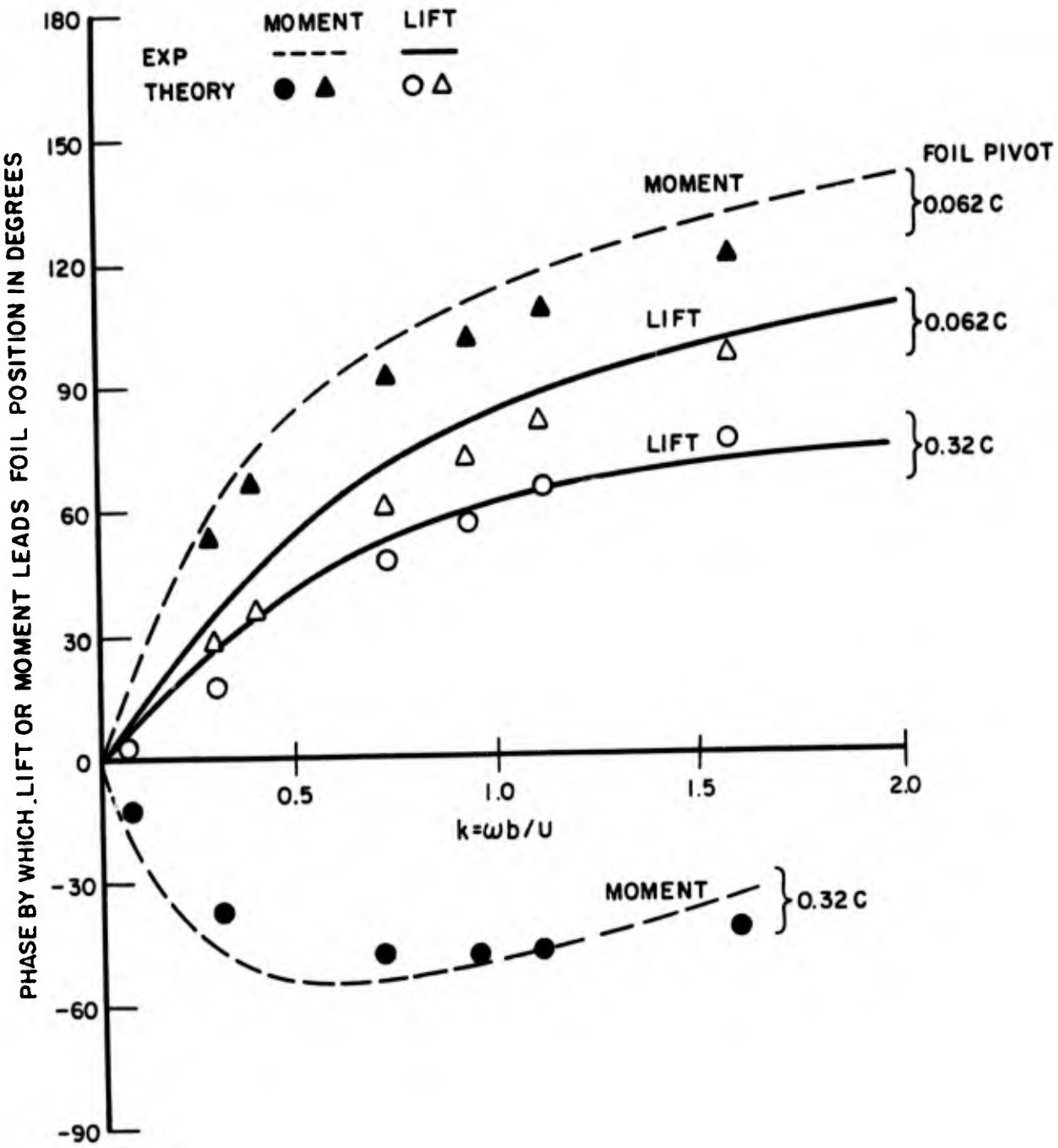

FIG. 12. THEORETICAL AND EXPERIMENTAL PHASES OF THE AG(EH) MAIN FOIL IN PITCHING MOTION

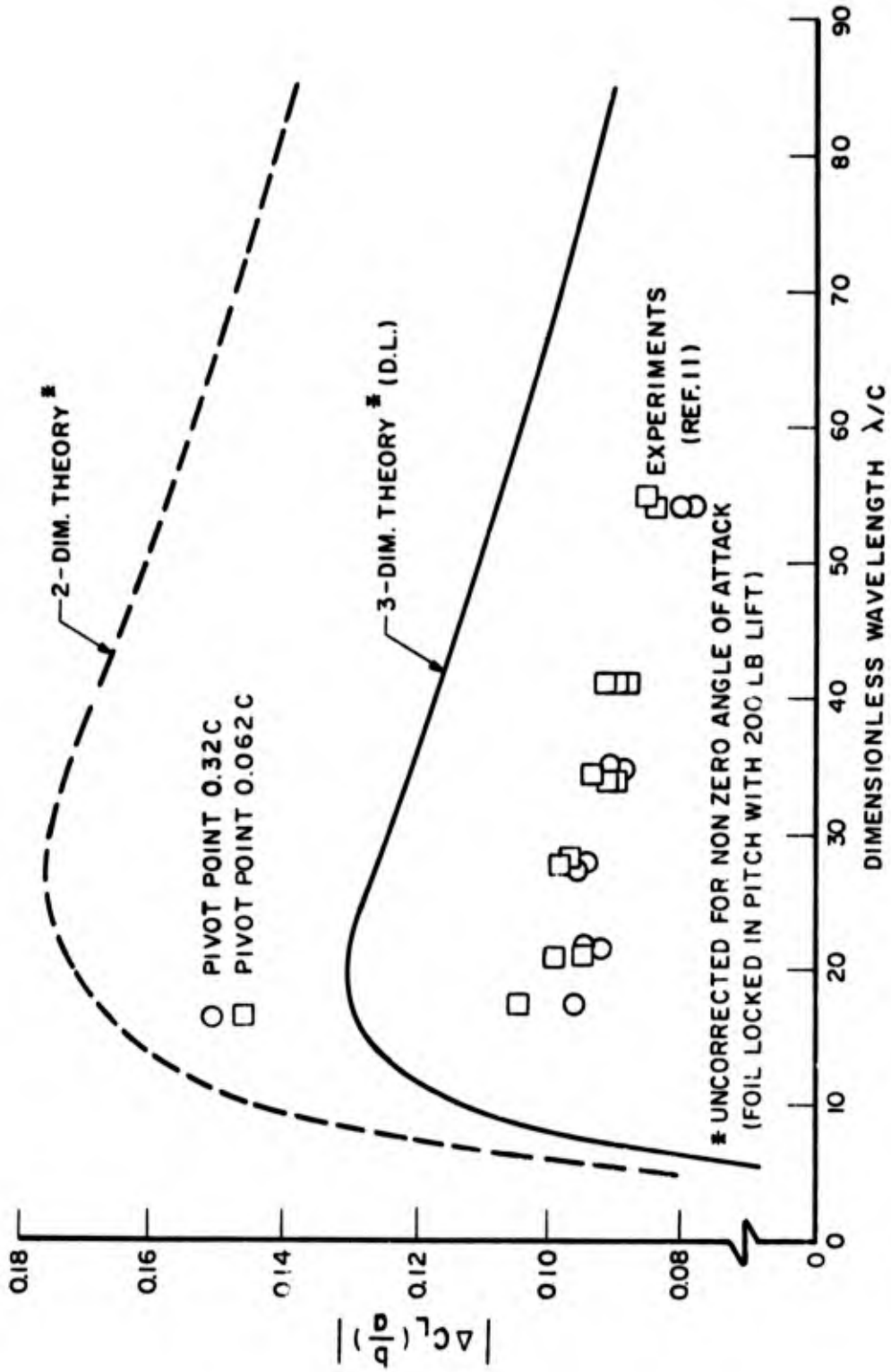

FIG.13. UNSTEADY LIFT RESPONSE OF THE AG (EH) MAIN FOIL IN REGULAR HEAD SEAS AT 14.2 KNOTS

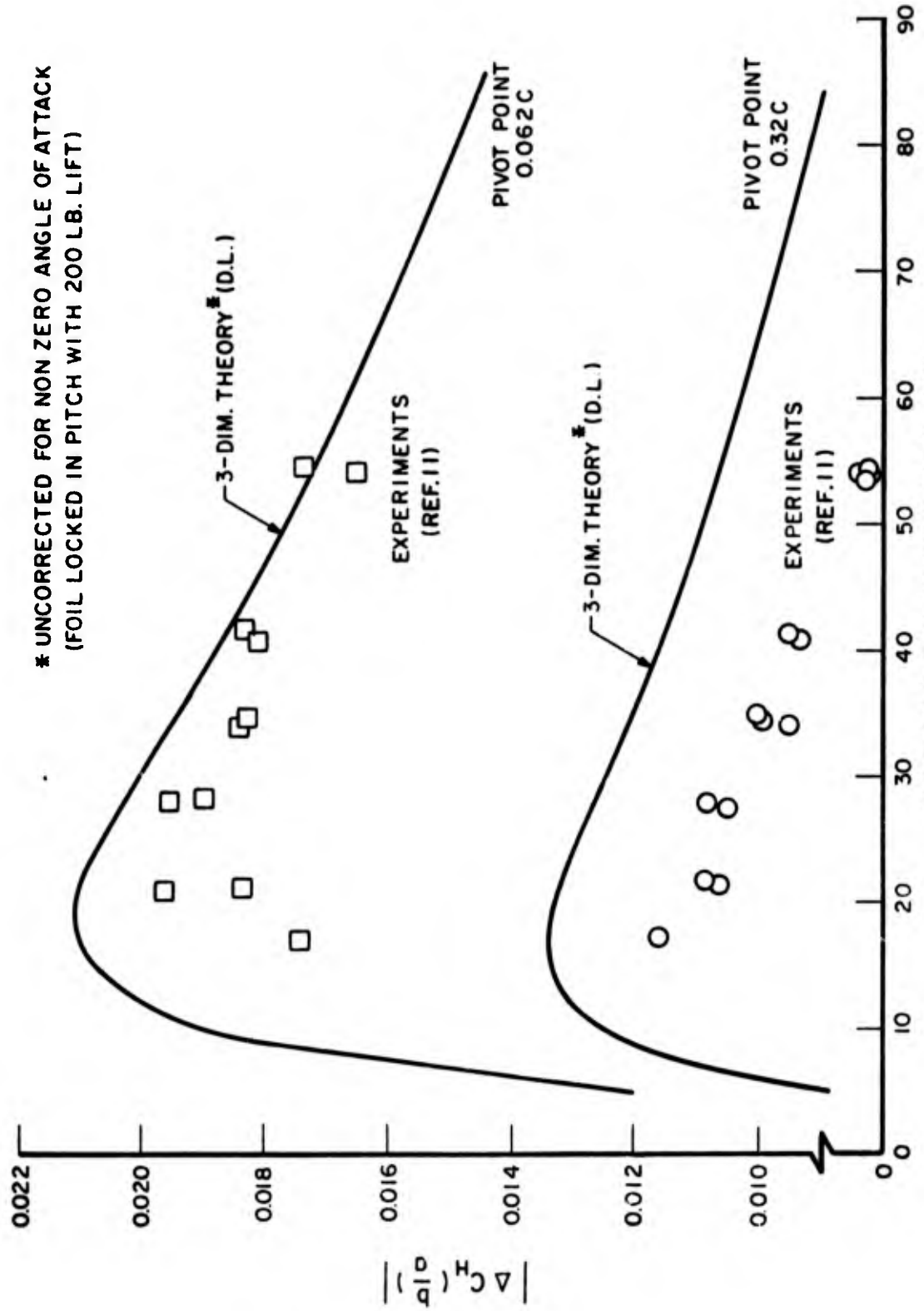

FIG. 14. UNSTEADY HINGE MOMENT RESPONSE OF THE AG (EH) MAIN FOIL IN REGULAR HEAD SEAS AT 14.2 KNOTS

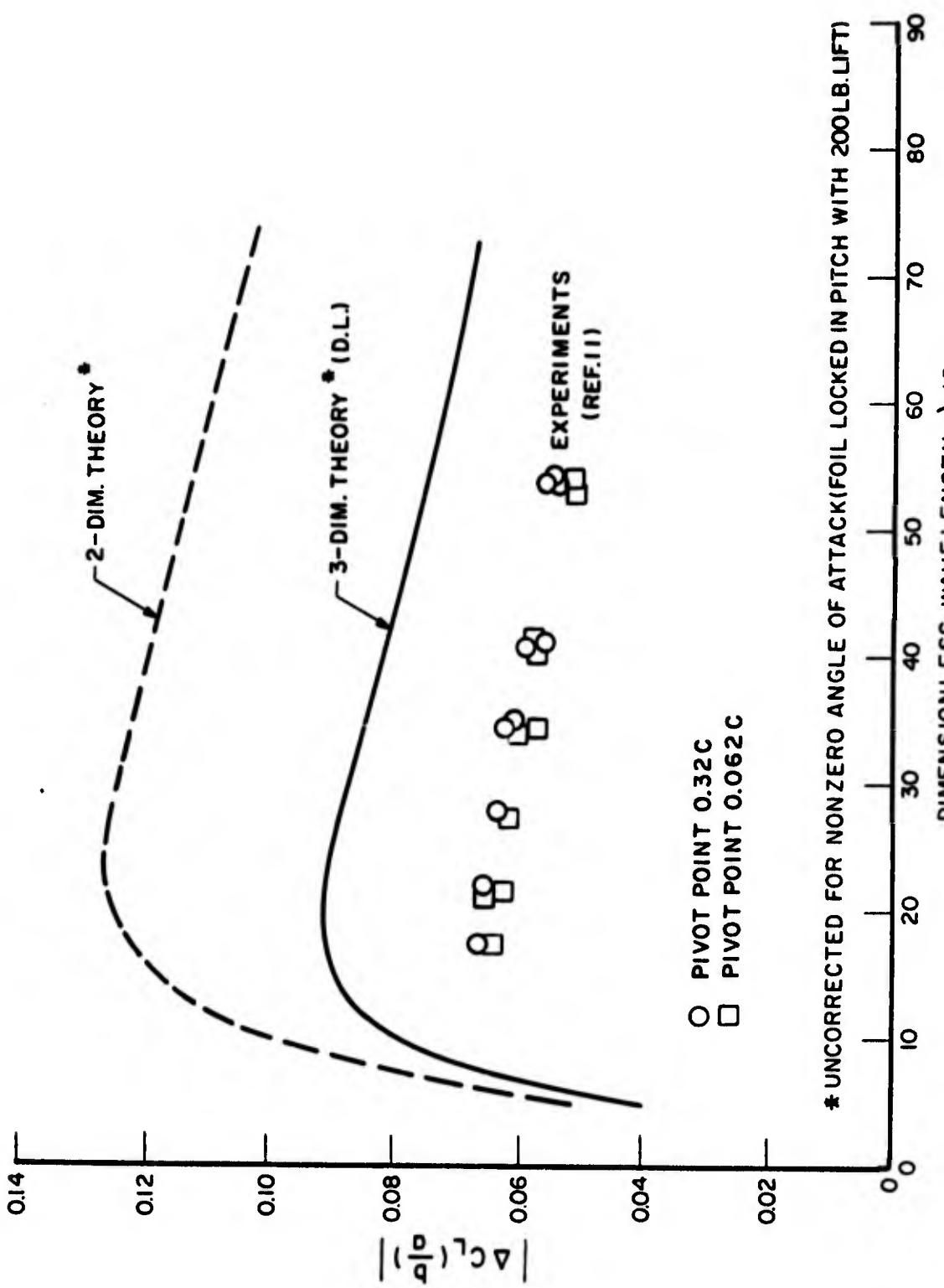

FIG. 15. UNSTEADY LIFT RESPONSE OF THE AG (EH) MAIN FOIL IN REGULAR HEAD SEAS AT 20.5 KNOTS

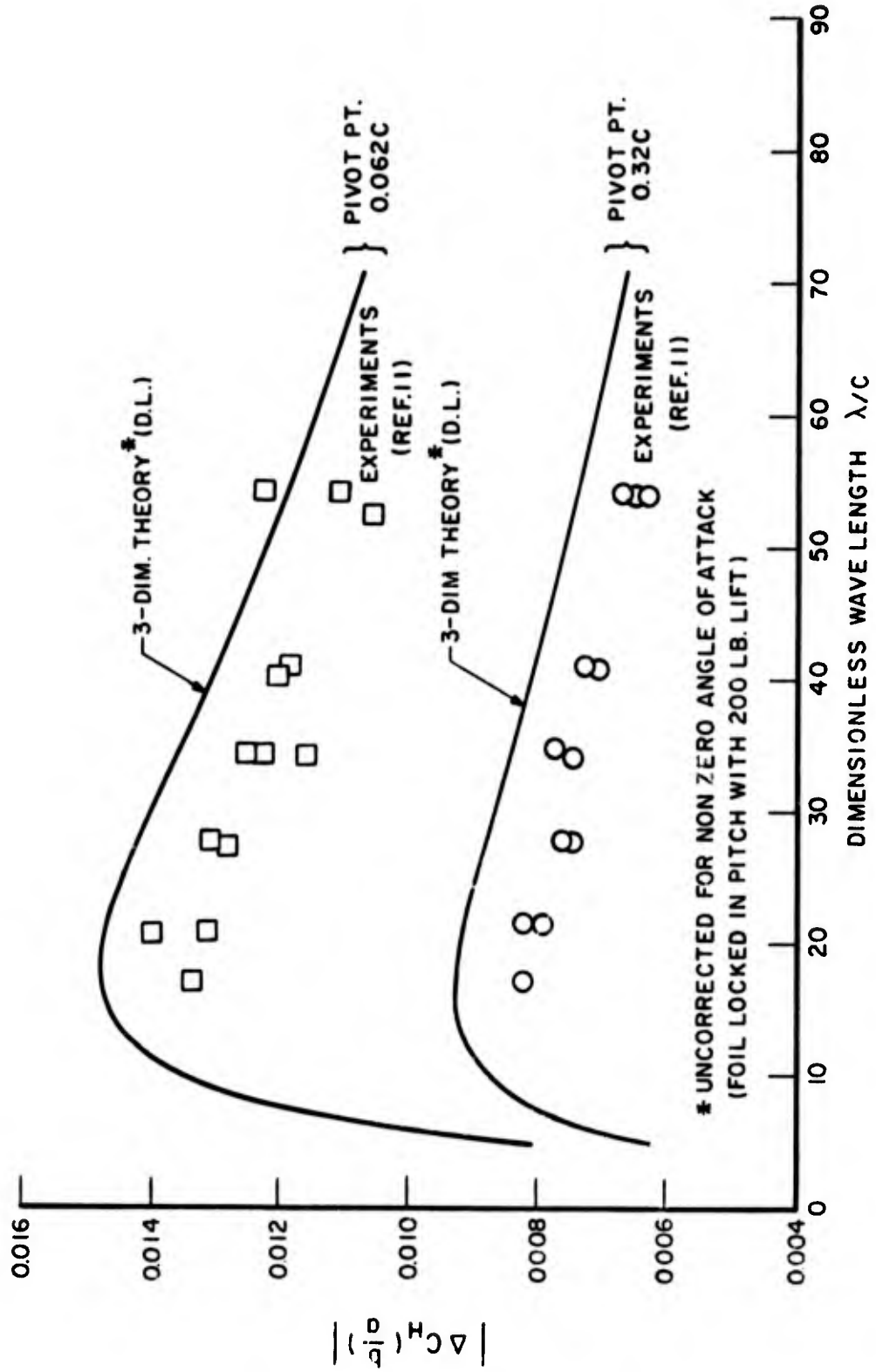

FIG. 16. UNSTEADY HINGE MOMENT RESPONSE OF AG(EH) MAIN FOIL IN REGULAR HEAD SEAS AT 20.5 KNOTS

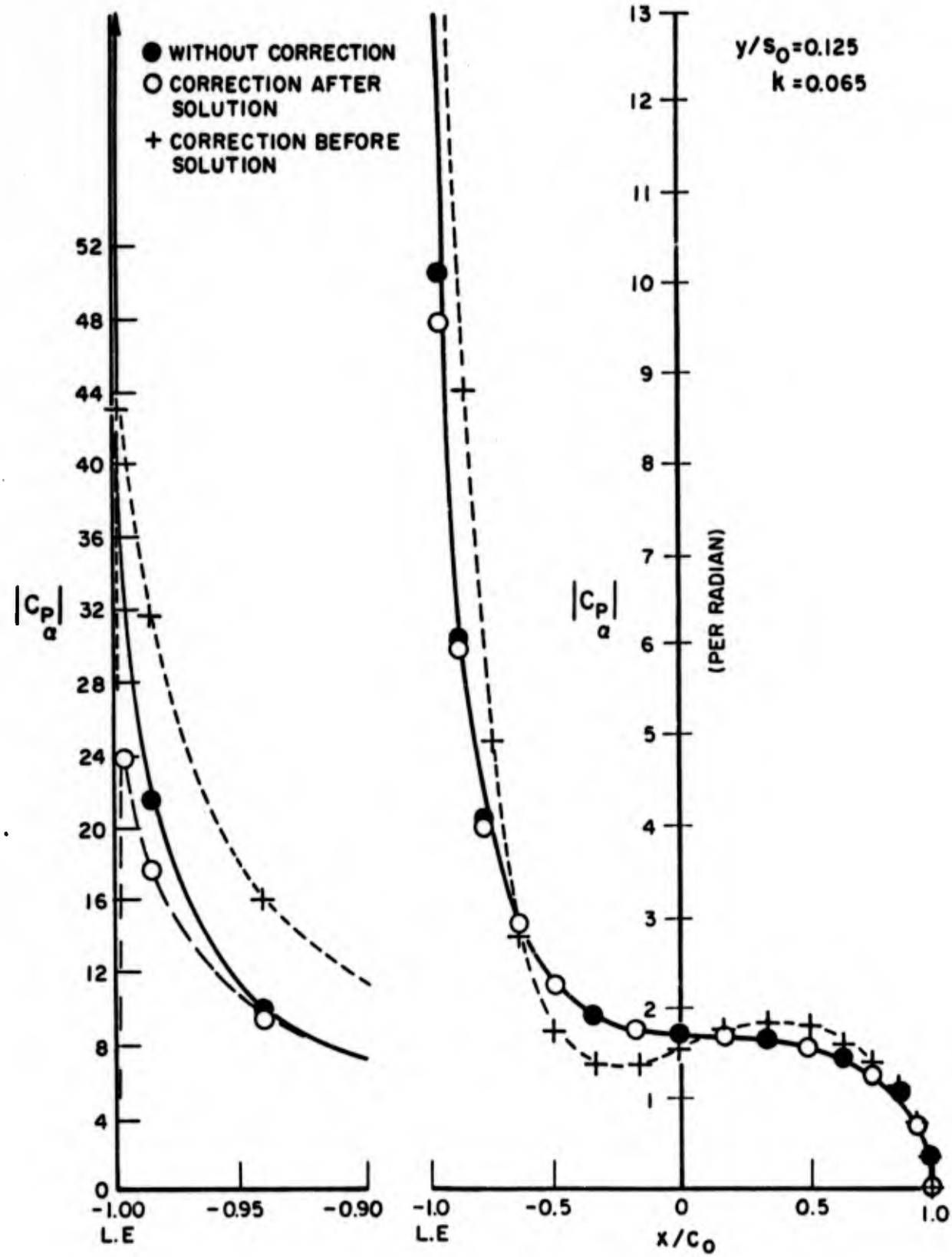

FIG. 17. CHORDWISE PRESSURE DISTRIBUTION FOR AG(EH) MAIN FOIL IN PITCHING MOTION OF UNIT AMPLITUDE (WITHOUT AND WITH CORRECTIONS FOR L.E. SINGULARITY)

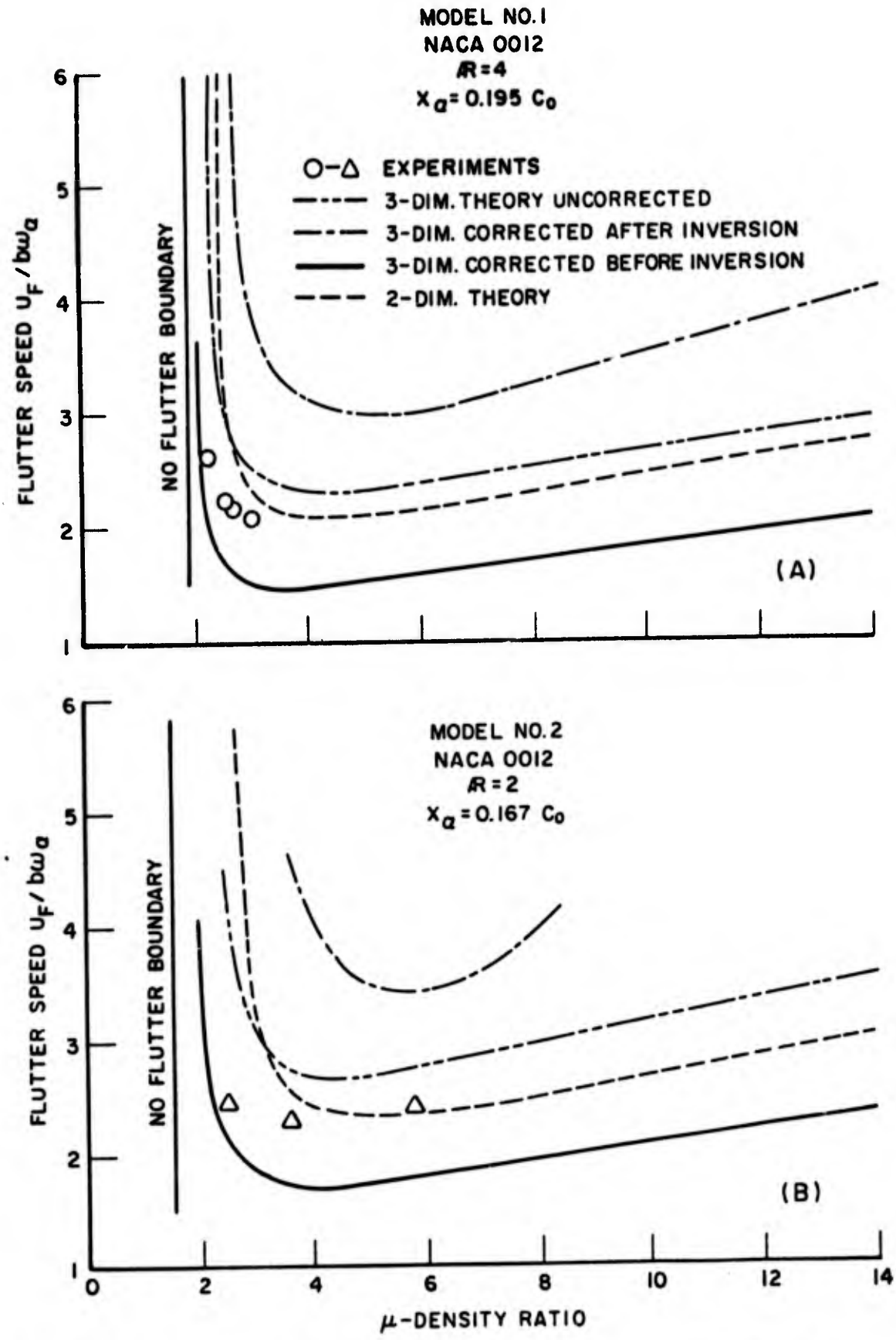

FIG. 18. COMPARISON OF EXPERIMENTAL FLUTTER SPEED WITH PREDICTIONS BY VARIOUS ANALYTICAL SCHEMES

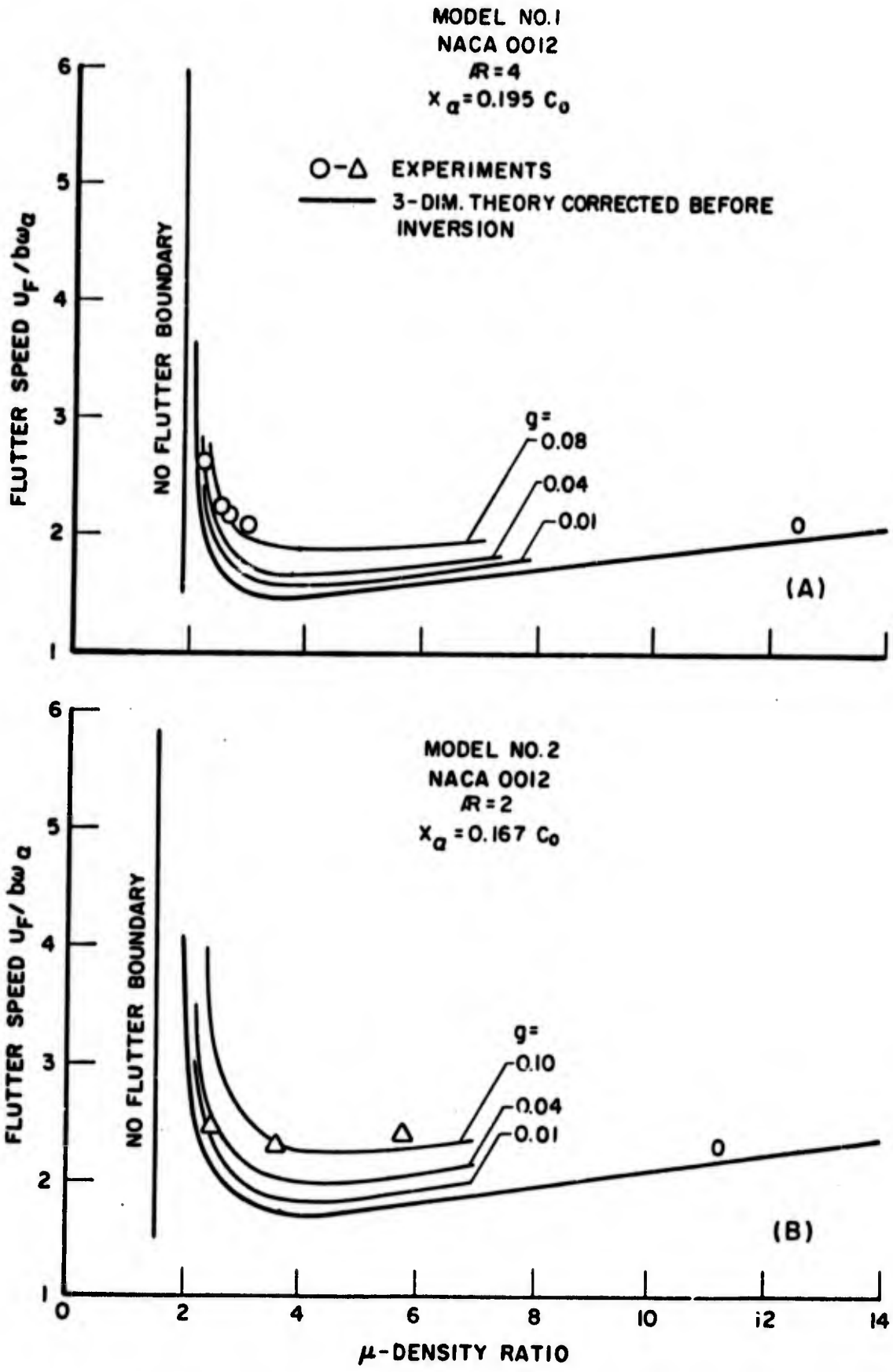

FIG. 19. COMPARISON OF EXPERIMENTAL FLUTTER SPEED WITH PREDICTIONS WITHOUT AND WITH STRUCTURAL DAMPING g

APPENDIX A

VALUES OF $I^{(\bar{m})}(f_1)$, $\Lambda^{(\bar{n})}(f_2)$ and $I_1^{(\bar{m})}(f_1)$ FOR VARIOUS $\bar{m}$ AND $\bar{n}$

$$I^{(\bar{m})}(f_1) = \frac{1}{\pi}\int_0^{\pi} \Phi(\bar{m}) e^{if_1\cos\phi}\, d\phi \qquad \text{(A-1)}$$

$$I^{(1)}(f_1) = \frac{1}{\pi}\int_0^{\pi} (1-\cos\phi) e^{if_1\cos\phi}\, d\phi = J_o(f_1) - iJ_1(f_1)$$

$$I^{(2)}(f_1) = \frac{1}{\pi}\int_0^{\pi} (1+2\cos\phi) e^{if_1\cos\phi}\, d\phi = J_o(f_1) + 2iJ(f_1)$$

$$I^{(\bar{m})}(f_1) = \frac{1}{\pi}\int_0^{\pi} \cos(\bar{m}-1)\phi\, e^{if_1\cos\phi}\, d\phi \quad \text{for } \bar{m} > 2$$

$$= i^{(\bar{m}-1)} J_{\bar{m}-1}(f_1)$$

where $J_n(f)$ is the Bessel function of the first kind.

$$\Lambda^{(\bar{n})}(f_2) = \frac{1}{\pi}\int_0^{\pi} \Theta(\bar{n}) e^{-if_2\cos\theta} \sin\theta\, d\theta \qquad \text{(A-2)}$$

$$\Lambda^{(1)}(f_2) = \frac{1}{\pi}\int_0^{\pi} \cot\frac{\theta}{2} \sin\theta\, e^{-if_2\cos\theta}\, d\theta = J_o(f_2) - iJ_1(f_2)$$

$$\Lambda^{(\bar{n})}(f_2) = \frac{1}{\pi}\int_0^{\pi} \sin(\bar{n}-1)\theta \sin\theta\, e^{-if_2\cos\theta}\, d\theta \quad \text{for } \bar{n} > 1$$

$$= \frac{(-i)^{\bar{n}-2}}{2}\left[J_{\bar{n}-2}(f_2) + J_{\bar{n}}(f_2)\right]$$

$$I_1^{(\bar{m})}(f_1) = \frac{1}{\pi}\int_0^{\pi} \Phi(\bar{m}) e^{if_1\cos\phi} \cos\phi d\phi \qquad \text{(A-3)}$$

$$I_1^{(1)}(f_1) = \frac{1}{\pi}\int_0^{\pi} (1-\cos\phi) e^{if_1\cos\phi} \cos\phi d\phi = -\frac{1}{2}[J_0(f_1) - J_2(f_1)] + iJ_1(f_1)$$

$$I_1^{(2)}(f_1) = \frac{1}{\pi}\int_0^{\pi} (1+2\cos\phi) e^{if_1\cos\phi} \cos\phi d\phi = [J_0(f_1) - J_2(f_1)] + iJ_1(f_1)$$

$$I_1^{(\bar{m})}(f_1) = \frac{1}{\pi}\int_0^{\pi} \cos(\bar{m}-1)\phi \; e^{if_1\cos\phi} \cos\phi d\phi \quad (\text{for } \bar{m} > 2)$$

$$= \frac{i^{\bar{m}-2}}{2}[-J_{\bar{m}}(f_1) + J_{\bar{m}-2}(f_1)]$$

All values for $(-f_1)$ are the complex conjugates of the foregoing expressions for $(+f_1)$.

APPENDIX B

TREATMENT OF THE SURFACE-PIERCING STRUT AT HIGH FROUDE NUMBER

A surface-piercing strut of length ℓ is moving in a steady flow at high speed in the positive x-direction, subjected to a velocity distribution W(x,z) as shown in Sketch 1.

Sketch 1

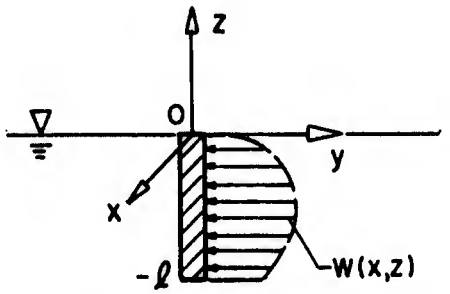

The integral equation relating the unknown loading distribution with the known velocity is given by (see Ref. 12)

$$W(x,z) = -\frac{1}{4\pi\rho Uc^2}\int_{\xi=-1}^{1} d\xi \int_{\zeta=-\ell/c}^{0} \Delta p(\xi,\zeta)K(x,z;\xi,\zeta)\,d\zeta \qquad \text{(B-1)}$$

where the kernel function is

$$K(x,z;\xi,\zeta) = \lim_{y-\eta\to o}\left(\frac{-\partial^2}{\partial y^2}\right)\int_{-\infty}^{x}\left\{\frac{1}{R_1}-\frac{1}{R_2}\right\}d\tau$$

$$R_1 = \{(\tau-\xi)^2 + (y-\eta)^2 + (z-\zeta)^2\}^{1/2}$$

$$R_2 = \{(\tau-\xi)^2 + (y-\eta)^2 + (z+\zeta)^2\}^{1/2}$$

and τ,x,y,z and ξ,η,ζ have been nondimensionalized with respect to chord c.

In addition, because of the high Froude number, the loading at the free surface must be considered nil, i.e.,

$$(\Delta p)_{\zeta=0} = 0$$

Now a vertical foil of length 2ℓ (see Sketch 2) is considered to be moving in an unbounded fluid at high speed and to be subjected to a known velocity distribution w(x,z).

Sketch 2

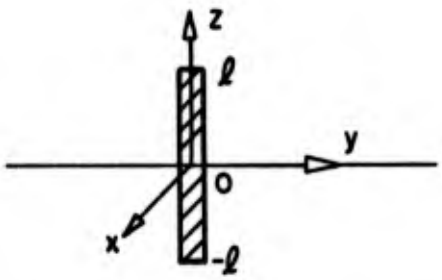

The corresponding integral equation relating the loading and the known velocity will be given by

$$w(x,z) = -\frac{1}{4\pi\rho Uc^2}\int_{-1}^{1} d\xi \int_{-\ell/c}^{\ell/c} \Delta p(\xi,\zeta)K(x,z;\xi,\zeta)d\zeta$$

$$= -\frac{1}{4\pi\rho Uc^2}\int_{-1}^{1} d\xi \left[\int_{-\ell/c}^{0} + \int_{0}^{\ell/c}\right]\Delta p(\xi,\zeta)K(x,z;\xi,\zeta)d\zeta \qquad \text{(B-2)}$$

where the kernel function is

$$\lim_{y-\eta\to 0}\left(\frac{-\partial^2}{\partial y^2}\right)\int_{-\infty}^{x}\frac{d\tau}{[(\tau-\xi)^2+(y-\eta)^2+(z-\zeta)^2]^{1/2}}$$

Making use of the transformation $\zeta = -\zeta'$ in the second integral of (B-2) yields

$$\int_{0}^{\ell/c}\Delta p(\xi,\zeta)K(x,z;\xi,\zeta)d\zeta = \int_{-\ell/c}^{0}\Delta p(\xi,-\zeta')K(x,z;\xi,-\zeta')d\zeta'$$

and imposing the condition

$$\Delta p(\xi,-\zeta') = -\Delta p(\xi,\zeta)$$

then

$$\int_{0}^{\ell/c}\Delta p(\xi,\zeta)K(x,z;\xi,\zeta)d\zeta = -\int_{-\ell/c}^{0}\Delta p(\xi,\zeta)K\ (x,z;\xi,-\zeta')d\zeta'$$

which, upon substitution into (B-2) yields

$$w(x,z) = -\frac{1}{4\pi\rho Uc^2}\int_{-1}^{1} d\xi \int_{-\ell/c}^{0}\Delta p(\xi,\zeta)\{K(x,z;\xi,\zeta) - K(x,z;\xi,-\zeta)\}d\zeta \qquad \text{(B-3)}$$

where $K(x,z;\xi,\zeta) = \dfrac{-\partial^2}{\partial y^2} \displaystyle\int_{-\infty}^{x} \frac{d\tau}{[(\tau-\xi)^2 + (y-\eta)^2 + (z-\zeta)^2]^{1/2}}$

and $K(x,z;\xi,-\zeta) = \dfrac{-\partial^2}{\partial y^2} \displaystyle\int_{-\infty}^{x} \frac{d\tau}{[(\tau-\xi)^2 + (y-\eta)^2 + (z+\zeta)^2]^{1/2}}$

Comparison of Eqs. (B-1) and (B-3) establishes the identity of integral equations (B-1) and (B-2), provided that use is made of the fact that the loading function satisfies the following relation

$$\Delta p(\xi,-\zeta) = -\Delta p(\xi,\zeta)$$

This can be accomplished by introducing a similar downwash or incident velocity distribution, viz.

$$w(x,-z) = -w(x,z) = -W(x,z)$$

Thus, it has been proved that a surface-piercing strut moving in a steady flow field at high Froude number, subjected to a known "downwash" distribution, behaves like a foil of double span immersed in an infinite fluid and subjected to a "downwash" distribution formed by extending the given distribution in antisymmetrical fashion with respect to the midlength.

It can be proved in a similar fashion that the surface-piercing strut moving at high Froude number in an unsteady flow field can be treated as a fully-submerged foil of twice the span of the strut subjected to a "downwash" distribution formed by extending the given distribution in antisymmetrical fashion with respect to the midlength.

LIFT ON A TWO-DIMENSIONAL AIRFOIL IN A TRAVELING GUST

In a traveling gust, the incident velocity distribution is given by

$$W(x)e^{i\omega t} = V_o e^{i(\omega t - \frac{2\pi x}{\lambda})} \tag{C-1}$$

which, after application of the generalized lift operator, becomes for each lift operator mode $\bar{m}$,

$$\bar{W}^{(m)} = \frac{1}{\pi}\int_o^\pi \phi(\bar{m})\ V_o e^{-i\frac{2\pi x}{\lambda}}\, d\phi$$

where $x = -b\cos\phi$ and b is semichord. Then

$$\bar{W}^{(\bar{m})} = V_o I^{(\bar{m})}(\tfrac{2\pi b}{\lambda}) \tag{C-2}$$

where $I^{(\bar{m})}(\frac{2\pi b}{\lambda})$ is as defined in Appendix A.

Reference 19 derives the two-dimensional counterpart of the integral equation

$$\bar{W}^{(\bar{m})} = \sum_{\bar{n}=1} L^{(\bar{n})}\ \bar{K}^{(\bar{m},\bar{n})} \tag{C-3}$$

and shows that in this case the kernel function $\bar{K}^{(\bar{m},\bar{n})}$ takes the following values for $\bar{m}$ and $\bar{n}$ from 1 to 3:

$\bar{m}$	$\bar{n}$	$\bar{K}^{(\bar{m},\bar{n})}\cdot\ [-2\pi\rho Ub]$
1	1	$A[J_o(k) - iJ_1(k)]$
1	2	$B[J_o(k) - iJ_1(k)] + \frac{i}{k}$
1	3	$C[J_o(k) - iJ_1(k)] - \frac{2i}{k} + \frac{4}{k^2}$
2	1	$A[J_o(k) + 2iJ_1(k)]$
2	2	$B[J_o(k) + 2iJ_1(k)] + \frac{i}{k}$
2	3	$C[J_o(k) + 2iJ_1(k)] + \frac{4i}{k} + \frac{4}{k^2}$

(C-4)

$$3 \quad 1 \quad A[-J_2(k)]$$

$$3 \quad 2 \quad B[-J_2(k)]$$

$$3 \quad 3 \quad C[-J_2(k)]$$

$$A = -ik[K_o(ik) + K_1(ik)] = -1/S(k)$$

$$B = K_1(ik) = C(k)/ikS(k)$$

$$C = 2[-\frac{2i}{k} K_1(ik) + K_o(ik)] = \frac{2i}{kS(k)} \{C(k) \ [1 + \frac{2i}{k}] - 1\}$$

where $k = \omega b/U$, $S(k)$ is Sears' function and $C(k)$ is the Theodorsen function. The following relation is also true

$$S(k) = C(k) \ [J_o(k) - iJ_1(k)] + iJ_1(k) \qquad \text{(C-5)}$$

For three $\bar{m}$ and $\bar{n}$ modes (C-3) is written as

$$L^{(1)}\bar{K}(1,1) + L^{(2)}\bar{K}(1,2) + L^{(3)}\bar{K}(1,3) = V_o[J_o(\frac{2\pi b}{\lambda}) - iJ_1(\frac{2\pi b}{\lambda})]$$

$$L^{(1)}\bar{K}(2,1) + L^{(2)}\bar{K}(2,2) + L^{(3)}\bar{K}(2,3) = V_o[J_o(\frac{2\pi b}{\lambda}) + 2iJ_1(\frac{2\pi b}{\lambda})] \qquad \text{(C-6)}$$

$$L^{(1)}\bar{K}(3,1) + L^{(2)}\bar{K}(3,2) + L^{(3)}\bar{K}(3,3) = V_o[-J_2(\frac{2\pi b}{\lambda})]$$

Making use of (C-4) and (C-5) in (C-6) yields the following solutions for $L^{(\bar{n})}$:

$$L^{(1)} = 2\pi\rho UbV_o\{C(k)[J_o(\frac{2\pi b}{\lambda}) - iJ_1(\frac{2\pi b}{\lambda})] + iJ_1(\frac{2\pi b}{\lambda})\}$$

$$L^{(2)} = 2\pi\rho UbV_o\{2iJ_1(\frac{2\pi b}{\lambda})[\frac{k}{2\pi b/\lambda} - 1]\} \qquad \text{(C-7)}$$

$$L^{(3)} = -\pi\rho UbV_o\{kJ_1(\frac{2\pi b}{\lambda}) - kJ_1(k) \ \frac{J_2(\frac{2\pi b}{\lambda})}{J_2(k)}\}$$

and, since the total lift is (see Eq. 15)

$$L = L^{(1)} + \frac{1}{2} L^{(2)}$$

$$L = 2\pi\rho U b V_o \{C(k)[J_o(\tfrac{2\pi b}{\lambda}) - iJ_1(\tfrac{2\pi b}{\lambda})] + i \frac{k}{2\pi b/\lambda} J_1(\tfrac{2\pi b}{\lambda})\} \qquad (C\text{-}8)$$

This is the same as the known analytical solution of Kemp[23] and is the negative of Leehey's formula[25] because of the difference in sign convention for lift L.

The moment about the midchord of a two-dimensional airfoil in a traveling gust is given by (cf Eq. 16a)

$$M_{1/2} = \frac{1}{\pi} \int_o^\pi \{L^{(1)}(1+\cos\theta) + \sum_{\bar{n}=2} L^{(\bar{n})} \sin(\bar{n}-1)\theta \sin\theta\}[-b\cos\theta]d\theta \qquad (C\text{-}9)$$

where $[-b\cos\theta]$ is the moment arm about the midchord. Therefore

$$M_{1/2} = \frac{-b}{\pi} \int_o^\pi \{L^{(1)}\cos\theta + L^{(1)}\cos^2\theta + L^{(2)}\sin^2\theta\cos\theta + L^{(3)}\sin 2\theta \sin\theta\cos\theta\}d\theta$$

$$= -b[\frac{L^{(1)}}{2} + \frac{L^{(3)}}{4}]$$

and since total lift L is

$$L = L^{(1)} + \frac{L^{(2)}}{2}$$

$$M_{1/2} = -b[\frac{L}{2} - \frac{L^{(2)}}{4} + \frac{L^{(3)}}{4}] \qquad (C\text{-}10)$$

On substituting the values from (C-7), the moment becomes, with $\kappa = 2\pi b/\lambda$,

$$M_{1/2} = \frac{-bL}{2} + b^2\pi\rho U V_o \{iJ_1(\kappa)[\frac{k}{\kappa} - 1] + \frac{k}{4}[J_1(\kappa) - \frac{J_1(k)}{J_2(k)} J_2(\kappa)]\}$$

$$= \frac{-b}{2} L + b^2\pi\rho U V_o \{iJ_1(\kappa)[\frac{k}{\kappa} - 1] + J_1(\kappa)[\frac{k}{4} - \frac{k}{2\kappa}\frac{J_1(k)}{J_2(k)}] + \frac{k}{4}\frac{J_1(k)}{J_2(k)} J_o(\kappa)]\} \qquad (C\text{-}11)$$

since $J_2(\kappa) = \frac{2}{\kappa} J_1(\kappa) - J_o(\kappa)$

Leehey's formula for the moment about the midchord of a two-dimensional airfoil in a traveling gust is

$$M_{-1/2} = \frac{bL}{2} + b^2\pi\rho U V_o \{iJ_1(\kappa)[\frac{k}{\kappa} - 1] + \frac{2}{\kappa} J_1(\kappa)[\frac{k}{\kappa} - 1] - J_o(\kappa)[\frac{k}{\kappa} - 1]\}$$

As $\kappa \to 0$, $J_o(\kappa) \to 1$, $J_1(\kappa) \to 0$ and $J_1(\kappa)/\kappa \to 1/2$. Therefore, for small κ, large wavelength λ, both formulas are equivalent. Also, in the special case of a stationary wave when $\kappa = k$, the second terms of both formulas vanish leaving

$$M_{1/2} = \mp \frac{bL}{2}$$

which signifies that the resultant lift L is acting through the quarter-chord point of the airfoil in the case of a stationary sinusoidal gust.

However, in general, there is a discrepancy between the formula for $M_{1/2}$ developed here and by Leehey, which is probably slight.

APPENDIX D

EVALUATION OF THE θ-INTEGRATIONS

1. The removal of the leading edge singularity before the inversion of the integral equation requires that the following integrals be evaluated.

$$\text{a)}\quad \Lambda^{(1)}(f) = \frac{1}{\pi}\int_0^{\pi} \frac{\sin^2\theta}{1+\rho_o-\cos\theta}\, e^{-if\cos\theta} d\theta$$

Let $1+\rho_o = \frac{1+\alpha^2}{2\alpha}$

where $\alpha = 1+\rho_o - \sqrt{2\rho_o+\rho_o^2}$

Then $\frac{1}{1+\rho_o-\cos\theta} = \frac{2\alpha}{1+\alpha^2-2\alpha\cos\theta}$

By the Gegenbauer expansion[30]

$$\frac{1}{1+\alpha^2-2\alpha\cos\theta} = \sum_{n=o}^{\infty} \alpha^n C_n^1(\cos\theta) \qquad \text{(D-1)}$$

Therefore

$$\Lambda^{(1)}(f) = \frac{2\alpha}{\pi}\sum_{n=o}^{\infty}\alpha^n \int_o^{\pi} \sin^2\theta\, e^{-if\cos\theta} C_n^1(\cos\theta) d\theta$$

$$= \frac{2\alpha}{\pi}\sum_{n=o}^{\infty}\alpha^n \frac{2\Gamma(\frac{3}{2})\Gamma(\frac{1}{2})\Gamma(2+n)(-i)^n}{n!\Gamma(2)}\frac{J_{n+1}(f)}{f}$$

$$= 2\sum_{n=o}^{\infty}(-i)^n(n+1)\,\alpha^{n+1}\frac{J_{n+1}(f)}{f} \qquad \text{(D-2)}$$

Since $|\rho_o - \sqrt{2\rho_o+\rho_o}| \ll 1$,

$$\alpha^{n+1} = (1+\rho_o-\sqrt{\rho_o+\rho_o^2})^{n+1} \sim 1 + (n+1)(\rho_o - \sqrt{2\rho_o+\rho_o^2}) + \frac{(n+1)n}{2!}(\rho_o-\sqrt{2\rho_o+\rho_o^2})^2$$

$$+ \frac{(n+1)(n)(n-1)}{3!}(\rho_o-\sqrt{2\rho_o+\rho_o^2})^3 \qquad \text{(D-3)}$$

Therefore

$$\Lambda^{(1)}(f) \sim 2\left\{\sum_{n=o}^{\infty}(-i)^n(n+1)\frac{J_{n+1}(f)}{f} + (\rho_o - \sqrt{2\rho_o+\rho_o^2})\sum_{n=o}^{\infty}(-i)^n(n+1)^2\frac{J_{n+1}(f)}{f}\right.$$

$$+\frac{(\rho_o - \sqrt{2\rho_o+\rho_o^2})^2}{2}\sum_{n=o}^{\infty}(-i)^n\, n(n+1)^2\frac{J_{n+1}(f)}{f}$$

$$\left.+\frac{(\rho_o - \sqrt{2\rho_o+\rho_o^2})^3}{6}\sum_{n=o}^{\infty}(-i)^n(n-1)(n)(n+1)^2\frac{J_{n+1}(f)}{f}\right.$$

or

$$\Lambda^{(1)}(f) \sim 2\left\{\sum_{n=o}^{\infty}(-i)^n(n+1)\frac{J_{n+1}(f)}{f} - \sqrt{2\rho_o+\rho_o}\sum_{n=o}^{\infty}(-i)^n(n+1)^2\frac{J_{n+1}(f)}{f}\right.$$

$$+\rho_o\sum_{n=o}^{\infty}(-i)^n(n+1)^3\frac{J_{n+1}(f)}{f} - \rho_o\frac{\sqrt{2\rho_o+\rho_o^2}}{3}\sum_{n=o}^{\infty}(-i)^n n(n+1)^2(n+2)\frac{J_{n+1}(f)}{f}$$

$$\left.+\rho_o^2\sum_{n=o}^{\infty}(-i)^n(n+1)^2n^2\frac{J_{n+1}(f)}{f} + O(\rho_o^{5/2}) + \ldots.\right. \qquad \text{(D-4)}$$

It can be shown that

$$2\sum_{n=o}^{\infty}(-i)^n(n+1)\frac{J_{n+1}(f)}{f} = \sum_{n=o}^{\infty}(-i)^n[J_n(f)+J_{n+2}(f)] = J_o(f) - iJ_1(f)$$

$$2\sum_{n=o}^{\infty}(-i)^n(n+1)^2\frac{J_{n+1}(f)}{f} = \sum_{n=o}^{\infty}(-i)^n(n+1)[J_n(f)+J_{n+2}(f)] = e^{-if}{}^{*} \qquad \text{(D-5)}$$

$$2\sum_{n=o}^{\infty}(-i)^n(n+1)^3\frac{J_{n+1}(f)}{f} = J_o(f) - 2f[J_1(f)+iJ_o(f)]$$

$$2\sum_{n=o}^{\infty}(-i)^n n(n+1)^2(n+2)\frac{J_{n+1}(f)}{f} = -3ife^{-if}$$

$$2\sum_{n=o}^{\infty}(-i)^n n^2(n+1)^2\frac{J_{n+1}(f)}{f} = -3ife^{-if} + 4f[J_1(f)+iJ_o(f)] + 2e^{-if} - 2J_o(f)$$

Then

---

*See Ref. 31, p. 196, Formula 94

$$\Lambda^{(1)}(f) \sim J_o(f) - iJ_1(f) - \sqrt{2\rho_o+\rho_o^2}\, e^{-if} + \rho_o[J_o(f)(1-i2f) - 2fJ_1(f)]$$

$$+ i\rho_o \sqrt{2\rho_o+\rho_o^2}\, fe^{-if} + \rho_o^2[(2-i3f)e^{-if} - 2J_o(f)\ (1-i2f) + 4fJ_1(f)] \quad \text{(D-6)}$$

b) For $\bar{n} = 2$,

$$\Lambda^{(2)}(f) = \frac{1}{\pi}\int_o^\pi \frac{\sin^2\theta(1-\cos\theta)}{1+\rho_o-\cos\theta} e^{-if\cos\theta} d\theta = \Lambda^{(1)}(f) - i\frac{\partial}{\partial f}\Lambda^{(1)}(f) \quad \text{(D-7)}$$

c) For $\bar{n} = 3$,

$$\Lambda^{(3)}(f) = \frac{1}{\pi}\int_o^\pi \frac{\sin 2\theta\, \sin\theta(1-\cos\theta)}{1+\rho_o-\cos\theta} e^{-if\cos\theta} d\theta$$

$$= \frac{2}{\pi}\int_o^\pi \frac{\sin^2\theta\cos\theta - \sin^2\theta\cos^2\theta}{1+\rho_o-\cos\theta} e^{-if\cos\theta} d\theta$$

$$= 2i\frac{\partial}{\partial f}\Lambda^{(1)}(f) + 2\frac{\partial^2}{\partial f^2}\Lambda^{(1)}(f) = 2i\frac{\partial}{\partial f}\Lambda^{(2)}(f) \quad \text{(D-8)}$$

d) For $\bar{n} = 4$,

$$\Lambda^{(4)}(f) = \frac{1}{\pi}\int_o^\pi \frac{\sin 3\theta\, \sin\theta(1-\cos\theta)}{1+\rho_o-\cos\theta} e^{-if\cos} d\theta \quad \text{(D-9)}$$

$$= \frac{1}{\pi}\int_o^\pi \frac{\sin^2\theta[-1+\cos\theta+4\cos^2\theta-4\cos^3\theta]}{1+\rho_o-\cos\theta} e^{-if\cos\theta} d\theta = -\Lambda^{(2)}(f) + 2i\frac{\partial}{\partial f}\Lambda^{(3)}(f)$$

2. Removal of the l.e. singularity after the solution of the integral equation requires evaluation of the foregoing integrals at f = 0.

a) From (D-2)

$$\Lambda^{(1)}(0) = 2\sum_{n=o}^{\infty}(-i)^n(n+1)\alpha^{n+1}\frac{J_{n+1}(f)}{f} = \sum_{n=o}^{\infty}(-i)^n\alpha^{n+1}[J_n(f)+J_{n+2}(f)]$$

evaluated at f = 0. The only contribution will be at n = 0. Therefore

$$\Lambda^{(1)}(0) = \alpha = 1 + \rho_o - \sqrt{2\rho_o+\rho_o^2} \quad \text{(D-10)}$$

This result can also be obtained by setting f = 0 in Equation (D-6).

b) From (D-7)

$$\Lambda^{(2)}(0) = \Lambda^{(1)}(0) - i \frac{\partial}{\partial f} \Lambda^{(1)}(f)\Big|_{f=0}$$

Since

$$-i \frac{\partial}{\partial f} \Lambda^{(1)}(f) = \frac{-i}{2} \sum_{n=o}^{\infty} (-i)^n \alpha^{n+1} [J_{n-1}(f) - J_{n+3}(f)]$$

when $f = 0$ only $n = 1$ will contribute. Therefore

$$\Lambda^{(2)}(0) = \alpha - \frac{1}{2}\alpha^2 = \frac{1}{2} - \rho_o - \rho_o^2 + \rho_o \sqrt{2\rho_o+\rho_o^2} \qquad \text{(D-11)}$$

c) From (D-8)

$$\Lambda^{(3)}(0) = \alpha^2 + 2i \frac{\partial}{\partial f} [-i \frac{\partial}{\partial f} \Lambda^{(1)}(f)]_{f=0}$$

where

$$2i \frac{\partial}{\partial f} [-i \frac{\partial}{\partial f} \Lambda^{(1)}(f)] = \frac{1}{2} \sum_{n=o}^{\infty} (-i)^n \alpha^{n+1} [J_{n-2}(f) - J_n(f) - J_{n+2}(f) + J_{n+4}(f)]$$

and, at $f = 0$, the only contributions are from $n = 0$ and $n = 2$. Then

$$2i \frac{\partial}{\partial f} [-i \frac{\partial}{\partial f} \Lambda^{(1)}(f)] = \frac{-\alpha}{2} - \frac{\alpha^3}{2}$$

Therefore

$$\Lambda^{(3)}(0) = \frac{-\alpha}{2}(1-2\alpha+\alpha^2) = \frac{-\alpha}{2}(\alpha-1)^2 = -\rho_o - 4\rho_o^2 - 2\rho_o^3 + 2(\rho_o+\rho_o^2)\sqrt{2\rho_o+\rho_o^2}$$

$$\sim -\rho_o - 4\rho_o^2 + 2\rho_o \sqrt{2\rho_o+\rho_o^2} \qquad \text{(D-12)}$$

d) In similar fashion, it can be shown from (D-9) that

$$\Lambda^{(4)}(0) = \frac{-\alpha^2}{2}(\alpha-1)^2 = -\rho_o - 9\rho_o^2 - 12\rho_o^3 - 4\rho_o^4 + (3\rho_o + 8\rho_o^2 + 4\rho_o^3)\sqrt{2\rho_o+\rho_o^2}$$

$$\sim -\rho_o - 9\rho_o^2 + 3\rho_o \sqrt{2\rho_o+\rho_o^2} \qquad \text{(D-13)}$$